

Electronic Theses and Dissertations, 2004-2019

2009

Characterization Of A Hydrogen-based Synthetic Fuel In A Shock Tube

Troy Flaherty
University of Central Florida

 Part of the [Mechanical Engineering Commons](#)
Find similar works at: <https://stars.library.ucf.edu/etd>
University of Central Florida Libraries <http://library.ucf.edu>

This Masters Thesis (Open Access) is brought to you for free and open access by STARS. It has been accepted for inclusion in Electronic Theses and Dissertations, 2004-2019 by an authorized administrator of STARS. For more information, please contact STARS@ucf.edu.

STARS Citation

Flaherty, Troy, "Characterization Of A Hydrogen-based Synthetic Fuel In A Shock Tube" (2009). *Electronic Theses and Dissertations, 2004-2019*. 4095.
<https://stars.library.ucf.edu/etd/4095>

CHARACTERIZATION OF A HYDROGEN-BASED
SYNTHETIC FUEL IN A SHOCK TUBE

by

TROY JUSTIN FLAHERTY
B.S. University of Central Florida, 2005

A thesis submitted in partial fulfillment of the requirements
for the degree of Master of Science
in the Department of Mechanical, Material, and Aerospace Engineering
in the College of Engineering
at the University of Central Florida
Orlando, Florida

Spring Term
2009

ABSTRACT

Shock-tube experiments were performed with syngas mixtures near atmospheric pressure with varying equivalence ratios behind reflected shock waves. Pressure and hydroxyl radical (OH^*) emission traces were recorded and used to calculate ignition delay time for a single mixture at equivalence ratios of $\Phi = 0.4, 0.7, 1.0,$ and 2.0 over a range of temperatures from $913 - 1803$ K. The syngas mixture was tested at full concentration as well as with 98% dilution in Argon. The full concentration mixtures were used to compare ignition delay time measurements with the theoretical calculations obtained through the use of chemical kinetics modeling using the Davis et al. mechanism. The dilute mixtures were used to study the OH^* emission profiles compared to those of the kinetics model. The model was in poor agreement with the experimental data especially at lower temperatures with an ignition delay difference of more than an order of magnitude. These ignition delay time data supplement the few existing data and are in relative agreement. The species profile comparison of OH^* compared to the model also showed poor agreement, with the worst agreement at the highest temperatures. While the disagreements with ignition delay time and profile comparisons cannot be explained at this time, the data presented support other findings. The data provide additional information towards understanding this disagreement relative to syngas mixtures despite the relatively well known kinetics of the primary constituents Hydrogen and Carbon Monoxide.

ACKNOWLEDGMENTS

A special thanks to Dr. Eric Petersen and the Gas Dynamics Research Group at the University of Central Florida including Chris Aul, Brandon Rotavera, Alex Barrett, Jaap de Vries, Joel Hall, Danielle Kalitan, Shatra Reehal, Mouna Lamnaouer, and Chris Zinner for their time and support.

TABLE OF CONTENTS

LIST OF FIGURES.....	vi
LIST OF TABLES.....	vii
LIST OF ABBREVIATIONS/NOMENCALTURE/ACRONYMS.....	viii
INTRODUCTION.....	1
Importance of Syngas.....	1
Objectives.....	4
BACKGROUND.....	9
Shock Tube Introduction.....	9
Contact Surface and Shock Front.....	10
Determination of Shock Parameters.....	11
Chemical Kinetics Modeling.....	11
OH* Chemiluminescence.....	13
Other Work.....	14
EXPERIMENT.....	17
Low Pressure Shock Tube.....	17
High Pressure Shock Tube.....	18
Experimental Calculation of Shock Parameters.....	19
Optical Diagnostic Techniques.....	20
Measurement of Ignition Delay Time.....	21
RESULTS.....	25
Summary of Test Conditions.....	25
Ignition Delay Time Results.....	26
Data Set 1 Results.....	28
Data Set 2 Results.....	29
Data Set 3 Results.....	30
Data Set 4 Results.....	31
Data Set 5 Results.....	32
Data Set 6 Results.....	33
DISCUSSION.....	35
Pre-Ignition.....	35
Species Profile Comparisons.....	38
Data Comparison to Other Work.....	42
CONCLUSIONS.....	45
APPENDIX A: MIX 19 RUN DATA.....	47
APPENDIX B: MIX 25 RUN DATA.....	50
APPENDIX C: MIX 32 RUN DATA.....	53
APPENDIX D: MIX 83 RUN DATA.....	56
APPENDIX E: MIX 87 RUN DATA.....	59
APPENDIX F: MIX 90 RUN DATA.....	62
APPENDIX G: SPECIES PROFILE COMPARISON.....	65
Mixture 19.....	66

Mixture 25.....	68
Mixture 32.....	70
LIST OF REFERENCES.....	72

LIST OF FIGURES

Figure 1: IGCC Flow Diagram [4]	2
Figure 2: Example pressure/emission traces for a concentrated fuel mixture	7
Figure 3: Example pressure/emission traces for a fuel mixture diluted in Argon	7
Figure 4: Generalized shock tube schematic with x-t diagram	9
Figure 5: Sample Chemkin species output.....	12
Figure 6: Typical emission trace with construction line for ignition time calculation	22
Figure 7: Typical endwall pressure trace.....	23
Figure 8: Typical sidewall pressure trace of a highly dilute mixture.....	24
Figure 9: Data set 1; Ignition delay time compared to modified Davis mechanism.	28
Figure 10: Data set 2; Ignition delay time compared to modified Davis mechanism.	29
Figure 11: Data set 3; Ignition delay time compared to modified Davis mechanism.	30
Figure 12: Data set 4; Ignition delay time compared to modified Davis mechanism.	31
Figure 13: Data set 5; Ignition delay time compared to modified Davis mechanism.	32
Figure 14: Data set 6; Ignition delay time compared to modified Davis mechanism.	34
Figure 15: Typical High Temperature Data	36
Figure 16: Typical Low Temperature Data Showing Pre-Ignition	36
Figure 17: OH* Profile Comparison at Low Temperature.....	37
Figure 18: Emission Data with Low Signal-to-Noise Ratio	39
Figure 19: OH* Species Comparison with Good Agreement.....	40
Figure 20: OH* Species Comparison with Poor Agreement.....	41
Figure 21: Comparison to Other Syngas Data of Similar Pressure	43

LIST OF TABLES

Table 1: Siemens Baseline Mixture; X_i is the mole fraction of species i	3
Table 2: Mixtures Used in the Current Research	4
Table 3: OH* Reactions and Rate Coefficients Added to Davis Mechanism	14
Table 4: Shock-Tube Run Data	26
Table 5: Ignition Delay Time Results.....	27

LIST OF ABBREVIATIONS/NOMENCALTURE/ACRONYMS

Atm: Atmosphere

A: Pre-exponential factor

E: Activation energy

Φ : Equivalence ratio of fuel to air

γ : Specific heat ratio (C_p/C_v)

HPST: High Pressure Shock Tube

IGCC: Integrated Gasification Combined Cycle

K: Kelvin

k: reaction rate

LPST: Low Pressure Shock Tube

M_1 : Mach number of incident shock

M_2 : Mach number of reflected shock

OH*: Hydroxyl in excited state (OH star)

P_1 : Initial pressure of driven section of shock tube

P_4 : Initial pressure of driver section of shock tube

P_5 : Pressure behind reflected shock wave

psia: pounds per square inch, absolute

ρ : Density

R: Gas constant

Syngas: Synthesis gas

T_1 : Initial temperature of driven section of shock tube

T_2 : Temperature of driven section after the passing of the incident shock wave

T_5 : Temperature behind reflected shock wave

T_{ign} : Ignition time

INTRODUCTION

Importance of Syngas

The energy crisis has become an increasingly popular topic over the past few decades. The world's dependence on oil has political, environmental, and economic implications. The current use of fossil fuels is cited as a primary contributor to economic issues, global warming, and military action. To reduce the dependence on a single commodity, many alternative fuels have been developed and implemented including hydrogen, biodiesel, ethanol, propane, natural gas, and the topic of this research, syngas.

Syngas is a gas that is primarily composed of hydrogen and carbon monoxide, and is most commonly formed by coal gasification. The term syngas is a general characterization of a CO/H₂ mixture which allows the ratio of hydrogen and carbon monoxide to vary. Even the presence of constituent gasses varies based on the process used to generate the gas and the geographic region in which the gas is produced [1].

With hundreds of possible variations of syngas, most research has been done on generalized CO/H₂ mixtures [2,3]. Little data exist for real syngas mixtures containing specific constituents outside of hydrogen and carbon monoxide. One objective of this research was to obtain data for a commercially used fuel mixture, rather than a pure CO/H₂ mixture.

Power generation companies are interested in syngas as an alternative fuel to meet government regulations, and position themselves for future technologies. Turbines can be combined with a coal gasification plant to form a cyclical process with a high return on electrical energy, with less environmental impact. Integrated Gasification Combined Cycle (IGCC) is the process which utilizes syngas for power generation as shown in Figure 1. Siemens Corporation in particular has developed this very process and continues funding research to improve and expand on the current capabilities.

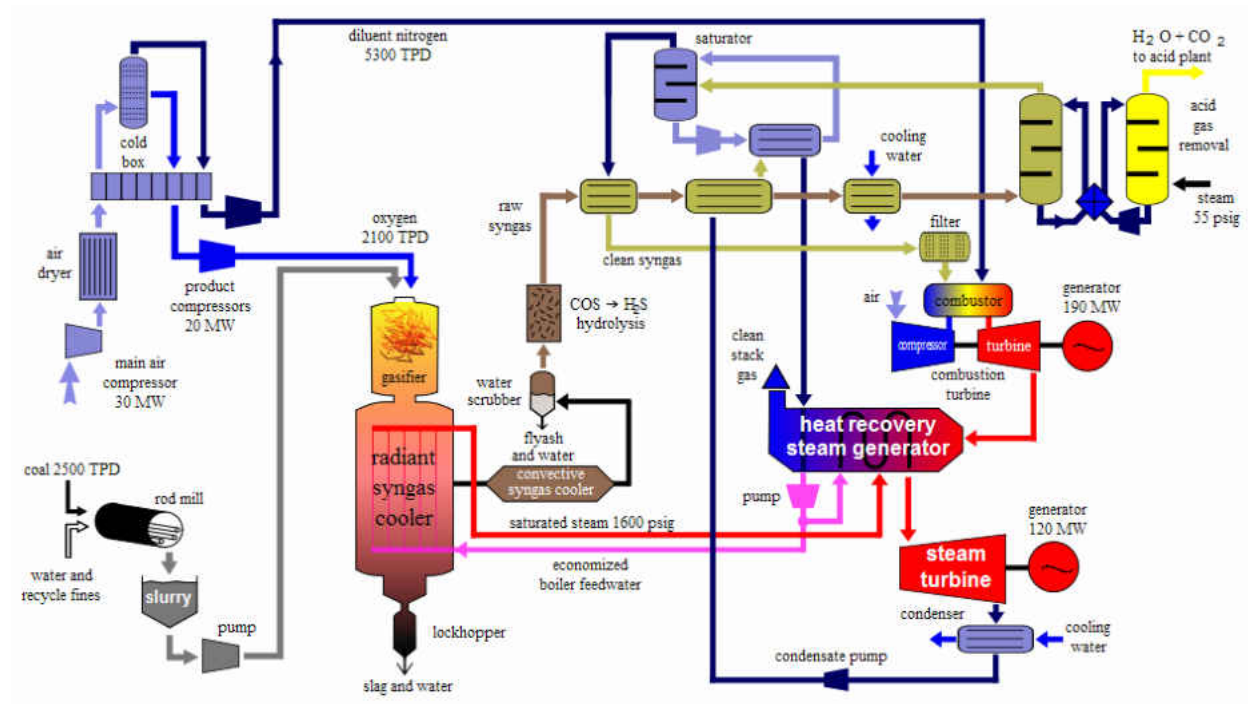


Figure 1: IGCC Flow Diagram [4]

Siemens has defined a particular mixture of syngas herein referred to as Siemens baseline mixture as shown in Table 1. Characterization of the Siemens baseline mixture is required to design and operate the combustor of a gas turbine. The ignition delay time is of primary focus because it is an indicator of the reactivity of the fuel, and a required parameter to operate a turbine.

Table 1: Siemens Baseline Mixture; X_i is the mole fraction of species i .

X_{H_2}	X_{CO_2}	X_{CO}	X_{CH_4}	X_{N_2}	X_{Ar}
0.776	0.102	0.044	0.038	0.030	0.010

This mixture is of particular interest to Siemens; however the findings from this single mixture have more general use when combined with existing data and compared to chemical kinetics models. The data obtained by the characterization of this fuel, combined with the data from several other variations, can be used to better predict the effects of varying ratios of hydrogen to carbon dioxide, as well as the effect of other constituents. All data obtained can be used to improve chemical kinetics models and allow for more accurate use of analytical models to predict combustion parameters.

Very little experimental data are available for complex fuel mixtures [5,6]. These data are needed to validate and/or improve existing chemical kinetics models which may not adequately predict ignition delay time. Many models extrapolate data from temperature and pressure ranges not similar to the conditions of an operating turbine. These existing models were also developed around specific fuel mixtures and make

assumptions on chemical reaction paths and rates [7]. The concentration of certain gases and the complexity of introducing other constituents may lead to errors in the chemical kinetic modeling.

Objectives

The objective of this research was to characterize the ignition properties of the Siemens baseline mixture by determining the ignition delay time for multiple equivalence ratios, over a range of temperatures, near atmospheric pressure. The mixtures used are listed in Table 2. Mixtures A, C, and D were run with the fuel at full concentration for accurate ignition delay time measurements. Mixtures A, B, and C were run at high levels of dilution with argon for improved time-dependent species concentration traces.

Table 2: Mixtures Used in the Current Research

Mixture	X_{H_2}	X_{CO_2}	X_{CO}	X_{CH_4}	X_{N_2}	X_{Ar}	X_{O_2}	Φ
A	0.114	0.015	0.007	0.006	0.678	0.001	0.179	0.4
B	0.180	0.024	0.010	0.009	0.614	0.002	0.161	0.7
C	0.233	0.031	0.013	0.012	0.561	0.003	0.147	1.0
D	0.359	0.047	0.021	0.018	0.438	0.004	0.113	2.0

Temperature behind the reflected shock wave was the primary independent variable. By varying the pressure of the low-pressure test region of the shock tube, the shock speed could be controlled. Higher pressure in the test region produces increased

resistance for the shock wave, slowing the shock speed. The temperature following the incident shock wave is then directly related to the shock speed by Equation 1 [8].

$$\frac{T_2}{T_1} = \frac{\left(\gamma M_1^2 - \frac{\gamma-1}{2}\right) \left(\frac{\gamma-1}{2} M_1^2 + 1\right)}{\left(\frac{\gamma+1}{2}\right)^2 M_1^2} \quad (1)$$

Gamma is the specific heat ratio and is a constant for monatomic gases. By plotting the above relation, it is evident that increasing the incident shock speed (M_1) increases the ratio of the temperature behind the shock wave (T_2) to initial temperature (T_1).

Combining this with the relationship between the shock speed and the pressure of the shock tube test region shows the inverse relation between the test region initial pressure and the change in temperature caused by the shock wave.

The temperature was varied for a single mixture of air and fuel to characterize that mixture. The process was then repeated for other mixtures, all with the same Siemens baseline fuel, but with varying equivalence ratios. This broadened the scope of the research and allowed for analysis of the ignition delay time in fuel rich and fuel lean environments as well as at stoichiometric equilibrium. The primary focus was with stoichiometric and fuel lean mixtures; however one fuel rich mixture was evaluated.

As previously mentioned, the mixtures were evaluated at full concentration as well as at high dilution with Argon. The concentrated runs are highly exothermic due to the

amount of fuel in the test region [9]. The timing of the reactions in the concentrated mixtures was easily observed using optical and mechanical devices as a very sharp rise in pressure or emission was observed. This sharp rise provided very accurate time-based data with little question as to the arrival of the shock wave and the onset of ignition.

The measurement devices are less accurate at plotting a complete time-based recording of the experiment at these high concentrations due to the sudden and large increase in signal due to the explosive nature of the ignition event in such mixtures. The optical devices can become saturated and display inaccurate results after the onset of ignition if the magnitude of the emission is too high. The pressure devices are subjected to a sudden impact and may be affected by vibrations or turbulence in the shock tube. For these reasons, to study the gas after the onset of ignition, the gas must be diluted in an inert gas such as Argon to reduce the optical and mechanical output of the reaction without chemically altering the reaction. The magnitude of the signals from the measurement devices is reduced and can be accurately recorded. The comparison of concentrated and dilute traces at similar conditions is shown in Figure 2 and Figure 3.

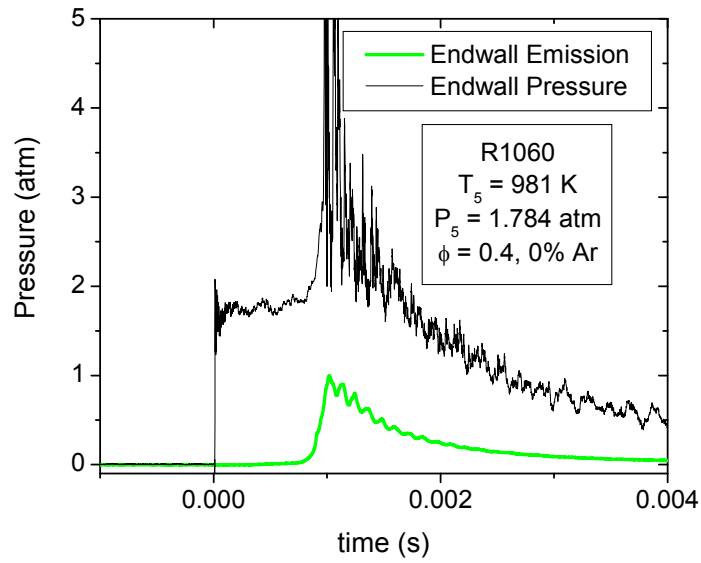


Figure 2: Example pressure/emission traces for a concentrated fuel mixture

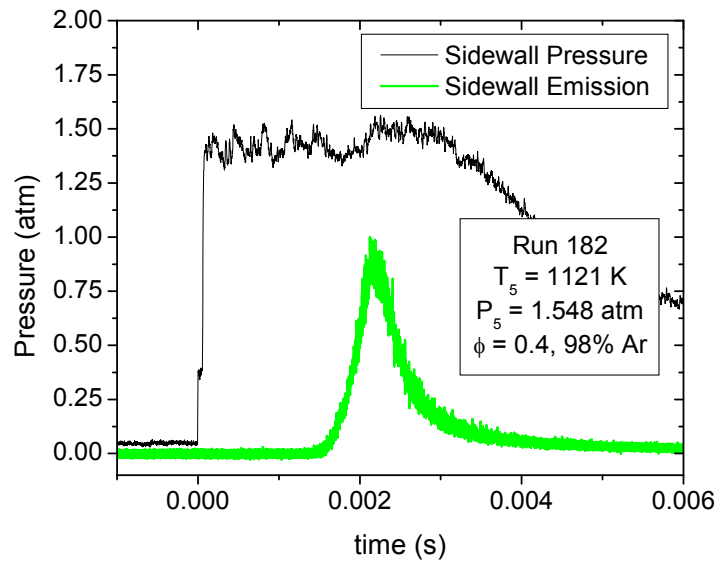


Figure 3: Example pressure/emission traces for a fuel mixture diluted in Argon

In parallel to running shock tube experiments, the reactions are modeled using chemical kinetics software [10] to predict the shock parameters and ignition delay time. After experiments are run and the data are reduced, the experimental data can be compared

to the kinetics models [7]. With this comparison, the model can either be validated for accuracy or analyzed for potential improvements.

BACKGROUND

Shock Tube Introduction

A generalized sketch of a shock tube is shown in Figure 4, along with a typical x-t diagram. This figure shows the interaction of the shock wave and expansion waves with respect to time and position along the shock tube.

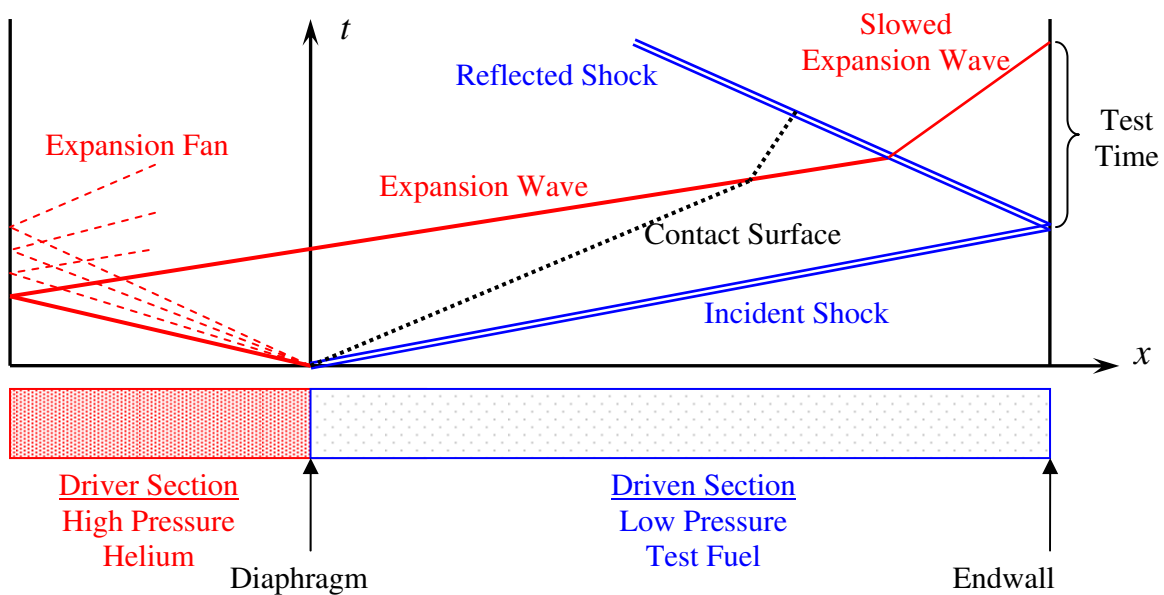


Figure 4: Generalized shock tube schematic with x-t diagram

A shock tube is comprised of two sections, a high-pressure driver section and a low-pressure driven section. The two sections are separated by a diaphragm. The

pressure differential between the two sections causes the diaphragm to burst, generating a shock wave that moves through the driven section. The shock wave creates a sharp rise in both temperature and pressure in the driven section. At the same time, an expansion wave is formed in the driver section which cools and reduces the pressure to eventually bring the entire shock tube to a steady state [8].

The shock tube is ideal for studying ignition because of the nearly instantaneous generation of known ignition conditions, holding these conditions stable for a period of time, and then sudden cooling to extinguish the ignition.

Contact Surface and Shock Front

As the diaphragm bursts, the driver and driven sections are now one continuous section, exposing the two gasses to each other. A contact surface is formed between the two gasses as the driver gas expands into the driven section. The contact surface moves into the driven section, compressing the gas with little mixing across the surface. If the contact surface is able to accelerate to a speed faster than the local speed of sound, a series of compression waves formed during the acceleration will combine to form a single shock front [8].

It is the shock front that causes a nearly instant increase in temperature and pressure in the driven gas section. The gas will remain at this constant elevated temperature and pressure between the shock front and the contact surface.

Determination of Shock Parameters

Applying ideal gas laws to one-dimensional reflected shock conditions yields the pressure relation shown in Equation 2 and the temperature relation shown in Equation 3 [8].

$$\frac{P_5}{P_1} = \left\{ \frac{2\gamma M_1^2 - (\gamma - 1)}{\gamma + 1} \right\} \left\{ \frac{(3\gamma - 1)M_1^2 - 2(\gamma - 1)}{(\gamma - 1)M_1^2 + 2} \right\} \quad (2)$$

$$\frac{T_5}{T_1} = \frac{\{2(\gamma - 1)M_1^2 + (3 - \gamma)\} \{(3\gamma - 1)M_1^2 - 2(\gamma - 1)\}}{(\gamma + 1)^2 M_1^2} \quad (3)$$

The above equations are complicated by the fact that the specific heat ratio (γ) is only constant for monatomic gases. The specific heat ratio is dependant on the chemical composition of the gas, temperature, and density. To perform this calculation, the Frosh program [11] is used to determine the temperature and pressure behind the reflected shock wave when accounting for changes in specific heats with temperature.

Chemical Kinetics Modeling

The chemical kinetics were modeled using the Shock subroutine of Chemkin [12]. Chemkin requires input from a thermodynamic file, chemical mechanism, shock

parameters, and composition of gas in test section. The output is the concentration with respect to time of any one of the intermediate species involved in the reaction. These data can be compared directly to the experimental data to validate/improve the mechanism rates and paths. A sample Chemkin species output is shown in Figure 5.

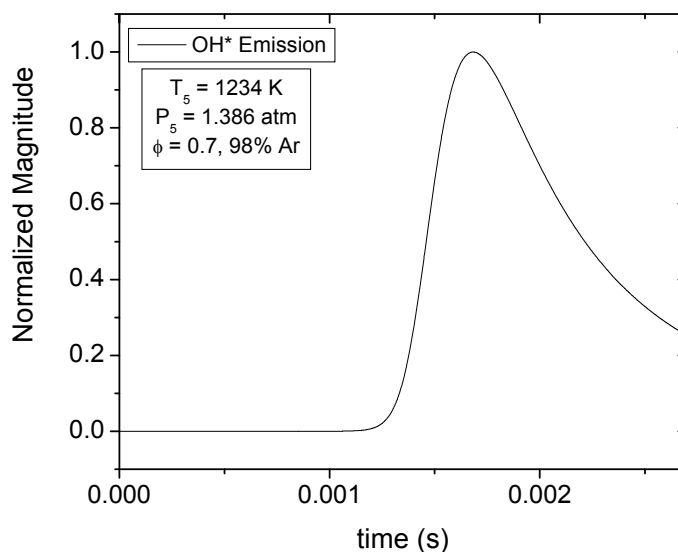


Figure 5: Sample Chemkin species output

The Davis et al. mechanism [7] was used for the kinetic modeling of the syngas mixture based on a study by Kalitan and Petersen [2]. It was shown that the Davis mechanism agreed with experimental data better than the GRI-Mech 3.0 [13] and Mueller et al. [14] mechanisms. The comparison was made using CO/H₂ mixtures near atmospheric pressure over a range of temperatures similar to those of this study.

OH* Chemiluminescence

OH chemiluminescence is the emission of light from excited OH, herein referred to as OH*. OH is a common marker of ignition delay time, however it is much easier to detect the light emission from OH* rather than direct measurement of OH. OH* can be measured using optical diagnostic techniques which are non-intrusive to the chemical reaction [15]. The initial rise time of OH* and OH coincide closely, which allows the use of either state to be used for accurate ignition delay time measurement [9,15,16].

Light is emitted from the OH radical in the ultraviolet spectrum near 307 nm [9]. This emission can be captured using a photomultiplier tube positioned to collect light from a window in the test region. The photomultiplier must be configured for the appropriate time response and filtered to receive only light emitted in the band near 307 nm.

OH* is the preferred diagnostic for measurement of ignition delay time [9], however when comparing to analytical data obtained from chemical kinetics modeling, OH* is not included in the Davis mechanism. To supplement the mechanism, the reactions listed in Table 3 were added [17]. The rate coefficient for each reaction is expressed as $k = AT^n e^{(-E/RT)}$ where E is the activation energy in cal/mol, R is the universal gas constant, and T is temperature in Kelvin.

Table 3: OH* Reactions and Rate Coefficients Added to Davis Mechanism

#	Reaction	A	n	E	Source
1	CH+O2=CO+OH*	3.24E+14	-0.4	4150	Hall and Petersen
2	H+O+M=OH*+M	3.10E+14	0.0	10000	Petersen et al.
3	OH*+AR=OH+AR	2.17E+10	0.5	2060	Hidaka et al.
4	OH*+H2O=OH+H2O	5.92E+12	0.5	-861	Smith et al.
5	OH*+CO2=OH+CO2	2.75E+12	0.5	-968	Smith et al.
6	OH*+CO=OH+CO	3.23E+12	0.5	-787	Smith et al.
7	OH*+H=OH+H	1.50E+12	0.5	0	Hidaka et al.
8	OH*+H2=OH+H2	2.95E+12	0.5	-444	Smith et al.
9	OH*+O2=OH+O2	2.10E+12	0.5	-482	Smith et al.
10	OH*+O=OH+O	1.50E+12	0.5	0	Hidaka et al.
11	OH*+OH=OH+OH	1.50E+12	0.5	0	Hidaka et al.
12	OH*+CH4=OH+CH4	3.36E+12	0.5	-635	Smith et al.
13	OH*=OH+hv	1.40E+06	0.0	0	Hidaka et al.
14	OH*+N2=OH+N2	1.08E+11	0.5	-1238	Hall and Petersen
15	H+OH+OH=OH*+H2O	1.45E+15	0.0	0	Smith et al.

Other Work

Other shock tube experiments using syngas mixtures have shown significant differences between the chemical kinetics models and the experimental data [2,5,6,18]. The discrepancy is important because syngas is primarily composed of Hydrogen and Carbon Monoxide, whose chemical kinetics are considered to be known and accurate [5]. Additional data are required of specific syngas mixtures to understand the effects of varying levels of Carbon Dioxide and other syngas constituents.

Lieuwen et al. reported the issues of fuel composition on combustor performance [19]. It was shown that the combustion properties of a fuel mixture cannot be inferred based on the properties of the individual constituents. Each constituent has its own reactivity,

flame speed, and flame temperature, and the mixture is not an average of these properties.

Lieuwen also reported the impact of diluents which change the specific heat, chemical kinetics rates, and the radiative heat transfer of the mixture. While these diluents are not primary reactants, they have a significant effect of the mixture performance. Flame speed and ignition delay time have a non-linear behavior with respect to fuel composition which is not currently completely understood [19].

Initial syngas data were presented by Petersen et al. [5] which showed a clear disagreement between the experimental data and the kinetics models at low temperatures. These data were obtained through three separate methods, rapid compression machine (RCM), flow reactor, and shock tube experiments. All three methods, conducted by different research facilities, showed the same disagreement compared to five different modern chemical kinetics models. It was also shown that the disagreement cannot be corrected with simple kinetic rate adjustments within the model [5]. Although these earlier-than-expected ignition events may not be completely driven by chemical kinetics, they do present a cause for concern when extrapolated to engine conditions which are far from the near-ideal situation in a shock tube experiment.

Additional CO/H₂ ignition delay time data were presented by Kalitan et al. [2,3] with various fuel lean CO/H₂ blends at atmospheric pressure. Kalitan reported a discrepancy between the kinetics models and experimental data at low temperatures by

as much as a factor of 5 and showed this was insensitive to small levels of impurities. Sensitivity analysis suggested that the mechanisms could be improved by adjusting the rates of the CO₂ forming reactions $\text{CO} + \text{O} + \text{M}$ and $\text{CO} = \text{H}_2\text{O}$ [3].

Shock tube ignition delay time data of the same mixture used in this work was performed by Reehal et al [6], also with similar discrepancies at low temperatures. This is the only other available data for a “real” syngas mixture in contrast to generic CO/H₂ mixtures. Reehal observed early pressure and emission increases prior to the main ignition event, however these anomalies were not indicative of poor model performance at the lower temperatures [6]. These pre-ignition events occurred at various temperatures with and without agreement with the model with respect to ignition delay time.

The relatively small amount of ignition delay time data for syngas all showed the same trend, with large disagreement at low temperatures compared to the kinetics models. While none of the papers could explain the discrepancy, there was a consistent request for additional data to better characterize syngas behavior at engine temperatures and pressures. To complement the existing data, the focus of this work was on “real” syngas mixtures at various equivalence ratios near atmospheric pressure both with and without Argon dilution.

EXPERIMENT

Two helium-driven shock tubes at the University of Central Florida Gas Dynamics Laboratory were used to determine ignition delay times for the experiments conducted in this research. A low-pressure shock tube was used to conduct the experiments using undiluted fuel-air mixtures. A high-pressure shock tube was used to achieve the sensitivity needed to characterize the fuel-air mixtures that were highly diluted in Argon. The details of the high pressure shock tube are discussed by Aul et al. [20] with a brief description of each shock tube provided here.

Low Pressure Shock Tube

The low pressure shock tube has a round Helium driver section with 7.6-cm internal diameter and 1.83-m length. The driven section has a 10.8-cm square cross-section with 4.27-m length between the diaphragm and the end wall. The two sections of the shock tube are separated by a ten thousandths of an inch Lexan diaphragm.

A Hamamatsu 1P21 photomultiplier tube (PMT) was used to capture light emission through optical windows located in the endwall and sidewall. A narrow-band filter was used to limit the light captured by the PMT to be centered about 307 nm for OH* emission. Four PCB 113A pressure transducers were used to record the passing of the incident shock wave. Combining these transducers with four Fluke model PM6666

interval counters, the shock speed could be measured. A single PCB 133A was used at the endwall to measure endwall pressure.

High Pressure Shock Tube

The high pressure shock tube was used to study the diluted fuel-air mixtures. It was used at similar temperature and pressure conditions as the low pressure shock tube. The naming convention is related to the conditions for which the shock tube was designed, not for the pressures tested in the experiments for this study.

The high pressure shock tube has a round driver section which has an internal diameter of 7.6 cm and length of 2.46 m. The driven section on the high pressure shock tube has an internal diameter of 15.2 cm and a length of 4.72 m. The two sections of the shock tube are separated by a breech-loaded diaphragm section [20]. Ten thousandths of an inch Lexan diaphragms were also used in the high pressure shock tube.

The same Hamamatsu PMT and bandpass filter were used for emission capture through sidewall optical ports. Shock speed was also recorded similarly, with the use of five PCB P113A pressure transducers spaced along the length of the driven section. The endwall pressure was measured using a single PCB 134A pressure transducer.

Experimental Calculation of Shock Parameters

The shock speed was calculated by measuring the time delay in the response between pressure transducers at known intervals along the length of the shock tube. As the shock wave passes these sensors, a timer was triggered to measure the time that elapses between the sensors. This discrete measurement of speed provided the average speed of the shock wave between the sensors.

Three to five sensors were used to obtain multiple velocity measurements in order to calculate the deceleration of the shock wave. This deceleration was needed to extrapolate the shock speed from the measurement locations to the shock tube endwall, which was the location of interest in the test section.

The sensors measured the initial passing of the shock wave after the rupture of the diaphragm which gave the speed of the incident shock wave. The second passing of the shock wave in the opposite direction, the reflected shock wave, was not measured directly. Reflected-shock parameters such as temperature and pressure behind the reflected shock wave could be derived from the incident shock speed using ideal gas laws [11].

The test conditions behind the reflected shock wave, temperature and pressure, were determined using the FROSH program [11]. By inputting the pressure and constituents of the gas in the driven section and the shock speed, the software used the shock tube

equations presented in the Background chapter, along with a thermodynamic database, Sandia [12], to determine the temperature and pressure behind the reflected shock wave [11].

Optical Diagnostic Techniques

Chemiluminescence was measured using a Hamamatsu 1P21 photomultiplier tube in a custom housing. The photomultiplier tube was filtered using a bandpass optical filter centered at 307 nanometers to measure the chemiluminescence of the hydroxyl radical (OH*). With the highly diluted mixtures, the emission was measured from the sidewall. The concentrated fuel-air mixtures were measured using endwall emission.

The use of sidewall emission was done to accommodate more accurate measurement of ignition time for the dilute mixtures. Endwall emission in undiluted fuel-air mixtures is an acceptable diagnostic tool due to the abrupt nature of the highly exothermic reaction. However, when using highly diluted mixtures the endwall emission technique produces artificially longer ignition delay time measurements due to the affect of ignition occurring at distances along the shock tube and not as a single event [21]. The high pressure shock tube was used for fuel-air mixtures diluted in approximately 98% Argon; therefore only sidewall emission diagnostics were used with this shock tube.

Measurement of Ignition Delay Time

Ignition was determined optically using the emission trace captured by the photomultiplier tube. The photomultiplier outputs a voltage which is recorded by a data acquisition system controlled by LabView software. To determine the onset of ignition, a linear fit was applied to the section of the emission trace with the largest positive slope. The intersection of this line with the zero emission axis is considered the onset of ignition for the purposes of this study and similarly in other related work [2,3,6,9,15-18].

The use of the onset time versus peak time for diagnostics was determined to be a more consistent approach for comparison to kinetics modeling by Hall [16]. This definition yields a measurement of ignition delay time that is consistent with other work, while being obtainable experimentally and analytically with repeatability.

An example emission trace with ignition time is shown in Figure 6. The intersection of the dashed green line, aligned with the steepest slope of the emission rise, with the initial zero emission value (x-axis) is the ignition time.

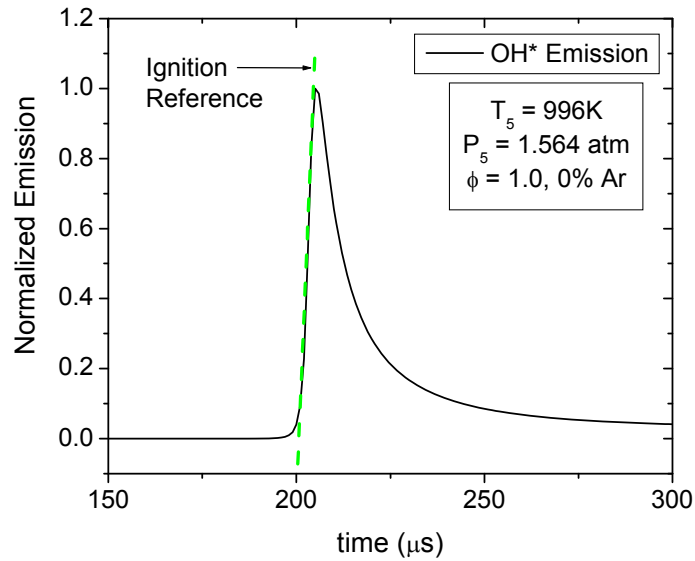


Figure 6: Typical emission trace with construction line for ignition time calculation

Ignition delay time is the time between the onset of the test conditions behind the reflected shock wave and the onset of ignition. The photomultiplier was used to determine the onset of ignition. However the time scale on the emission output is not aligned with time zero of the test conditions. The pressure trace was used to provide the necessary offset.

A pressure transducer, aligned with the optical measurement location, was used to determine time zero. For the dilute mixtures, this pressure transducer was on the sidewall aligned with the side window location. For concentrated mixtures, the transducer was located at the endwall. The endwall pressure trace showed a single pressure rise. The sidewall pressure trace showed the incident shock wave and a second pressure rise caused by the reflected shock wave. The reflected shock wave raises the gas to the temperature and pressure required for ignition. It is this second

rise that was used to determine time zero relative to the sidewall emission for ignition delay time measurements.

An example endwall pressure trace is shown in Figure 7. The first rise denotes the arrival of the shock wave at approximately 95 microseconds. The second rise that occurs around 300 microseconds is caused by the ignition. The endwall measurements were used for the concentrated fuel-air mixtures, which are highly exothermic. In this case the ignition delay time could be computed from the endwall pressure trace alone.

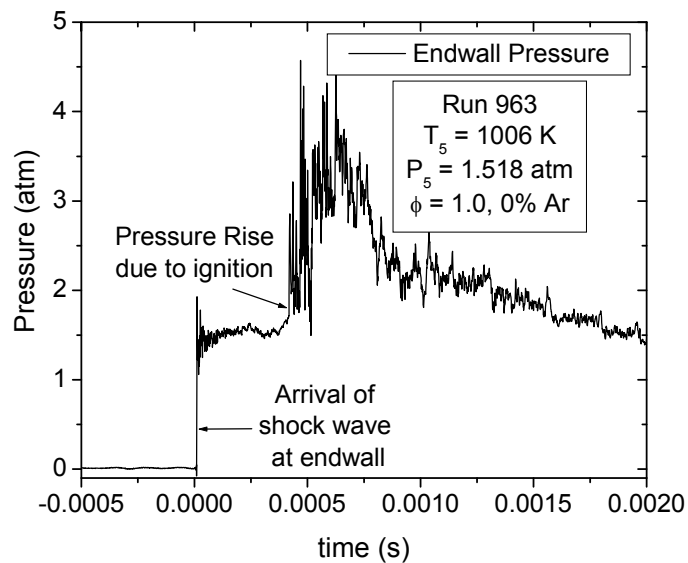


Figure 7: Typical endwall pressure trace

An example sidewall pressure trace is shown in Figure 8. The incident shock wave is shown at approximately zero seconds on the time scale and has a magnitude of approximately 25% of the total pressure rise. The pressure maintains this level for approximately 60 microseconds and then rises to a higher value. This is the arrival of

the reflected shock wave, and the relative constant pressure behind it. The sidewall pressure was used for dilute mixtures which do not have a large exothermic reaction. A pressure rise caused by ignition was not as evident as in the endwall pressure trace of a concentrated mixture as was shown in Figure 7.

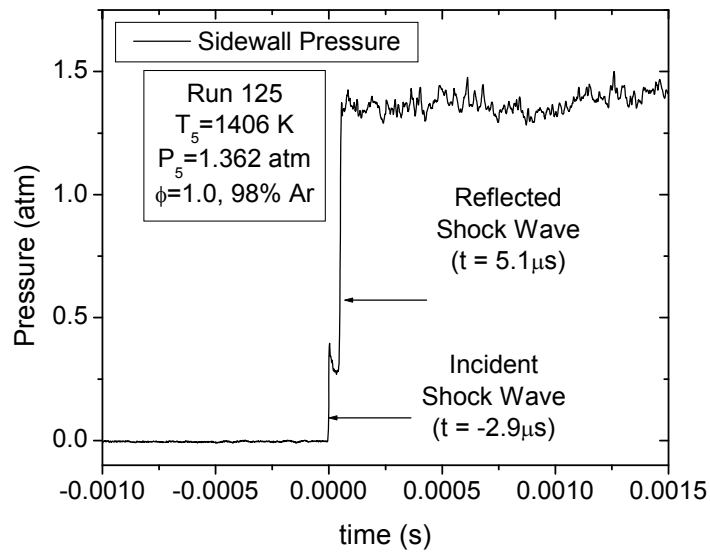


Figure 8: Typical sidewall pressure trace of a highly dilute mixture

RESULTS

This chapter presents the results obtained from shock tube experiments of the Siemens baseline syngas mixture compared to the Davis mechanism modified for OH* modeling. The Siemens baseline mixture was run at multiple equivalence ratios; stoichiometric ($\Phi=1.0$), fuel lean ($\Phi=0.4$ and $\Phi=0.7$), and fuel rich ($\Phi=2.0$). The experiments were performed with full concentration of fuel in the test section and repeated with the fuel diluted in 98% Argon.

Summary of Test Conditions

There were a total of 6 sets of data from the combinations of equivalence ratios and levels of dilution. The data sets are summarized in Table 4, showing the shock tube used, equivalence ratio, argon dilution level, average pressure and average temperature behind the reflected shock. The mixture numbers listed in the table and shown in the figures were those assigned per the laboratory log for a particular shock tube. Pressure and emission traces obtained for each run are provided in Appendices A through F.

Table 4: Shock-Tube Run Data

Data Set	Tube Run #	UCF Shock Tube	Mixture (Ref Table 2)	Equiv. Ratio (Φ)	Ar Dilution	$P_{5,avg}$ (atm)	Temp Range (K)
1	19	HPST	C	1.0	98%	1.43	1045-1667
2	25	HPST	A	0.4	98%	1.42	1072-1803
3	32	HPST	B	0.7	98%	1.37	1040-1464
4	83	LPST	C	1.0	0%	1.42	935-1222
5	87	LPST	D	2.0	0%	1.38	923-1065
6	90	LPST	A	0.4	0%	1.71	967-1123

The average pressure across all data sets is roughly 1.5 atm due to the size of diaphragm used in the shock tube. For each combination of equivalence ratio and dilution, the shock tube runs covered a range of temperatures from as high as 1803 K to as low as 923 K.

Ignition Delay Time Results

The ignition delay times were obtained experimentally and compared to the Davis mechanism [7] using the Chemkin [10] Shock subroutine with the Sandia thermodynamic database [12]. The Davis mechanism was modified to include the optimized reactions for predicting OH* [17]. Since the added reactions only affect the excited state, there are no changes to the predictions of the mechanism, other than the added capability pertaining to OH*. The ignition delay times from the experiments and mechanism results are listed in Table 5.

Table 5: Ignition Delay Time Results

Dilute Mixtures (98% Ar)					Concentrated Mixtures (0% Ar)				
Data Set	T (K)	P (atm)	T _{ign} (μs) Experiment	T _{ign} (μs) Model	Data Set	T (K)	P (atm)	T _{ign} (μs) Experiment	T _{ign} (μs) Model
1	1667	1.330	145	292	4	1152	1.332	65	47
	1406	1.362	370	648		1113	1.388	100	59
	1296	1.344	670	1027		1037	1.502	209	111
	1252	1.410	780	1195		1006	1.518	454	175
	1182	1.409	1080	1717		996	1.564	586	216
	1138	1.450	1450	2158		977	1.536	1042	379
	1073	1.520	1950	3180		935	1.405	2490	14490
	1045	1.616	2700	3750					
2	1803	1.257	147	244	6	1123	1.571	43	54
	1646	1.315	207	351		1073	1.662	63	79
	1507	1.335	64	518		1039	1.697	97	116
	1437	1.431	339	609		1015	1.698	243	171
	1301	1.359	591	1087		1002	1.744	330	232
	1217	1.487	1081	1451		983	1.754	670	496
	1121	1.548	1724	2385		981	1.784	888	621
	1072	1.633	2486	2880		967	1.766	1173	4469
3	1464	1.270	257	573	5	1065	1.267	90	95
	1410	1.376	356	638		1024	1.298	136	147
	1387	1.417	403	677		990	1.340	303	252
	1307	1.308	522	1010		971	1.365	493	421
	1297	1.316	586	1052		950	1.870	861	1626
	1269	1.299	687	1208		938	1.417	1218	6510
	1234	1.386	959	1338		930	1.465	1701	12725
	1189	1.432	1380	1624		923	1.396	1478	20919
	1138	1.450	2194	2146		913	1.438	1887	39975

Data Set 1 Results

Data set 1 utilized the UCF high pressure shock tube to obtain experimental data of the Siemens baseline mixture at an equivalence ratio of 1.0 diluted in 98% Argon. The average pressure over the 8 runs was 1.43 atm, and the experiments covered a temperature range of 1045 K – 1667 K. The experimental data are plotted in Figure 9 with a comparison to the Davis mechanism.

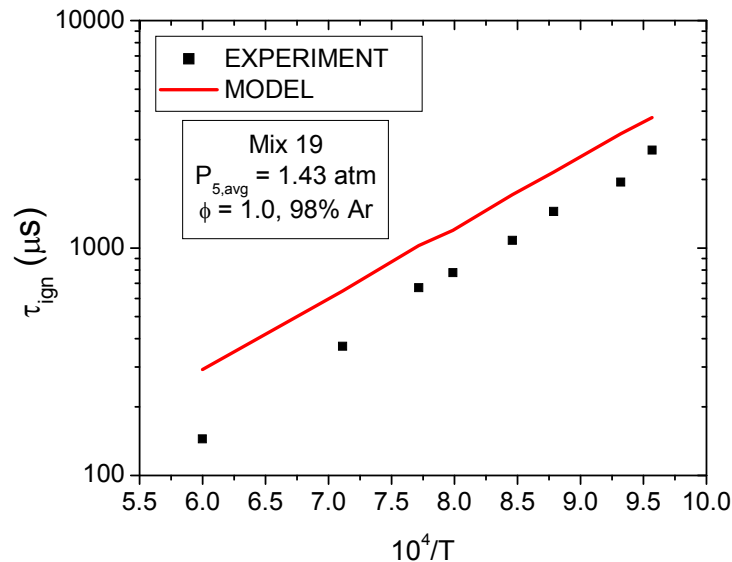


Figure 9: Data set 1; Ignition delay time compared to modified Davis mechanism.

For data set 1, the model over predicts the ignition delay time by a factor of 2. This relation is present across the temperature range tested. Despite the offset, the experimental data follow the slope of the model well, with slightly improved agreement at the lower end of the temperature range tested.

Data Set 2 Results

Data set 2 utilized the UCF high pressure shock tube to obtain experimental data of the Siemens baseline mixture at an equivalence ratio of 0.4 diluted in 98% Argon. The average pressure over the 8 runs was 1.42 atm, and the experiment covered a temperature range of 1072 K – 1803 K. The experimental data are plotted in Figure 10 with a comparison to the Davis mechanism.

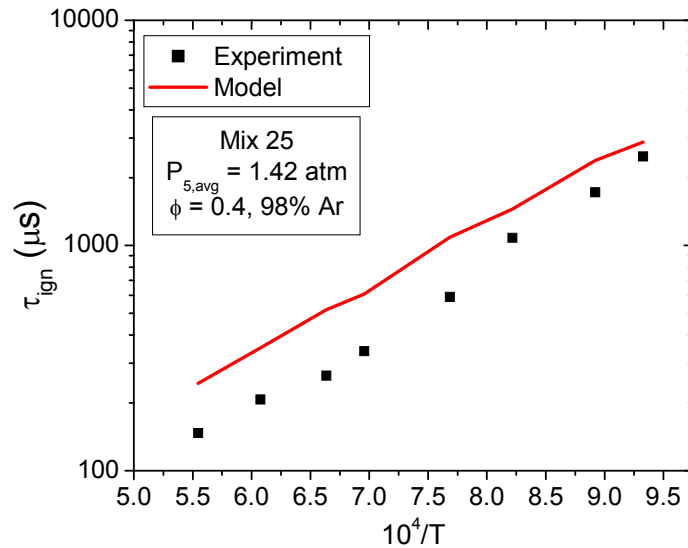


Figure 10: Data set 2; Ignition delay time compared to modified Davis mechanism.

The model over predicts the ignition time compared to the experimental data by approximately 100 μs across the temperature range. There is a difference in slope in which the percent error between the model and experimental data is reduced at the high end of the temperature range (~1800 K) showing the consistent 100 μs difference.

Data Set 3 Results

Data set 3 utilized the UCF high pressure shock tube to obtain experimental data of the Siemens baseline mixture at an equivalence ratio of 0.7 diluted in 98% Argon. The average pressure over the 9 runs was 1.37 atm, and the experiments covered a temperature range of 1040 K – 1464 K. The experimental data are plotted in Figure 11 with a comparison to the Davis mechanism.

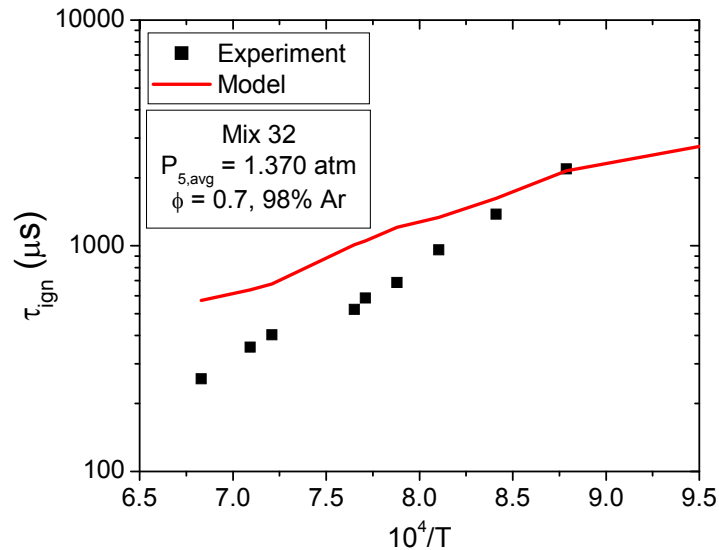


Figure 11: Data set 3; Ignition delay time compared to modified Davis mechanism.

The experimental data and model have roughly the same order of magnitude, but are otherwise dissimilar. The model over predicts ignition delay time by approximately 200 μs across the temperature range. At the high end of the temperature range (1250 K – 1450 K) the model and experimental data converge, with the experimental data slightly

over predicting the model at 1138 K. The results are limited by the total test time allowed by the shock tube physical features, preventing comparison below 1138 K.

Data Set 4 Results

Data set 4 utilized the UCF low pressure shock tube to obtain experimental data of the Siemens baseline mixture at an equivalence ratio of 1.0 without Argon dilution. The average pressure over the 7 runs was 1.42 atm, and the experiments covered a temperature range of 935 K - 1222 K. The experimental data are plotted in Figure 12 with a comparison to the Davis mechanism.

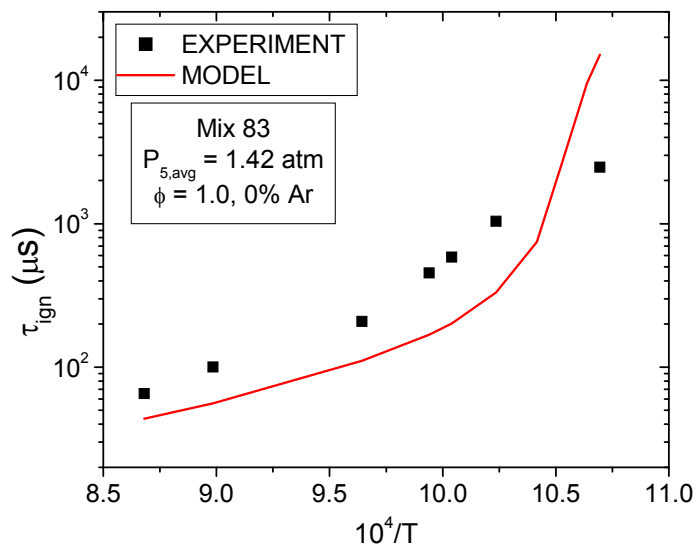


Figure 12: Data set 4; Ignition delay time compared to modified Davis mechanism.

The model under predicts the experimental data at the high end of the temperature range from about 960 K to 1220 K. Below 960 K, the model has a change in

temperature dependence and shows a sharp increase in ignition time where the model begins to over predict the experimental data. The experimental data show a similar change in temperature dependence, however the magnitude of change is much less and it occurs below 1030 K. In general, there is poor agreement between the experimental data and the model.

Data Set 5 Results

Data set 5 utilized the UCF low pressure shock tube to obtain experimental data of the Siemens baseline mixture at an equivalence ratio of 2.0 without Argon dilution. The average pressure over the 8 runs was 1.38 atm, and the experiment covered a temperature range of 923 K - 1065 K. The experimental data are plotted in Figure 13 with a comparison to the Davis mechanism.

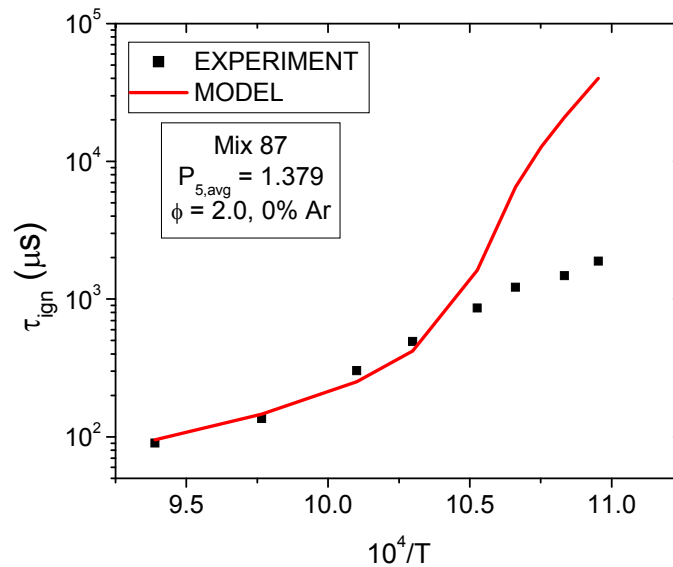


Figure 13: Data set 5; Ignition delay time compared to modified Davis mechanism.

For this fuel rich data set, the model agrees very well with the experimental data at the higher temperatures above 980 K. Below 980 K, the model shows a significant change in temperature dependence in which the model over predicts the experimental data by more than an order of magnitude at 930 K. The experimental data show no significant change in temperature dependence across the temperature range tested.

Data Set 6 Results

Data set 6 utilized the UCF low pressure shock tube to obtain experimental data of the Siemens baseline mixture at an equivalence ratio of 0.4 without Argon dilution. The average pressure over the 8 runs was 1.71 atm, and the experiments covered a temperature range of 967 K - 1123 K. The experimental data are plotted in Figure 14 with a comparison to the Davis mechanism.

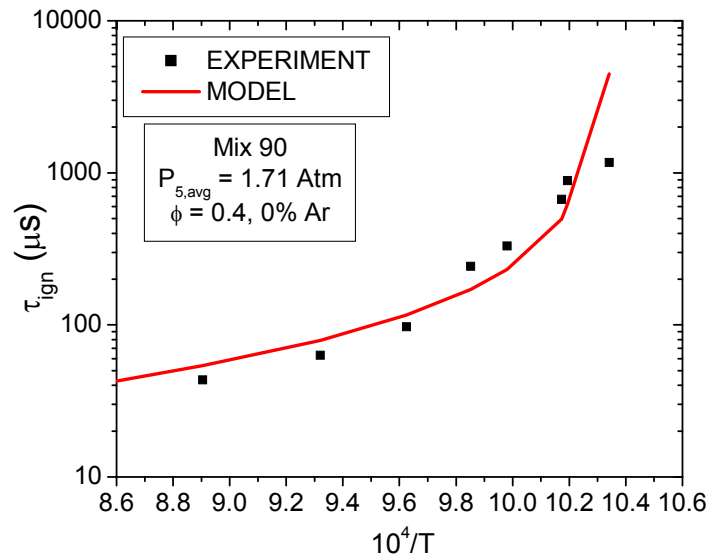


Figure 14: Data set 6; Ignition delay time compared to modified Davis mechanism.

The model agrees well with the experimental data for data set 6. The model slightly over predicts the ignition time compared to the experimental data above 1030 K. Between 980 K and 1030 K, the model under predicts the ignition time; however the final data point at 967 K is significantly accelerated compared to the model. The experimental data show a slight change in temperature dependence below 1030 K, while the model shows a much more significant change below 980 K.

DISCUSSION

In this section, the experimental data are further evaluated to discuss possible explanations for inconsistencies between the model and data obtained. The OH* species profile is discussed to show the presence of pre-ignition and other time-based differences. The data from this work are also compared to similar syngas data obtained by other researchers.

Pre-Ignition

All mixtures showed a large discrepancy between the experimental ignition delay times versus those calculated with the kinetics model at low temperatures. The concentrated fuel mixtures (no Argon dilution) were faster than the model by an order of magnitude or more below approximately 975 K as previously shown in Figures 12 through 14. This trend can be attributed to pre-ignition events by comparing the high temperature and low temperature results of a given data set.

Data set 4 was a concentrated fuel mixture with an equivalence ratio of 1.0 (data set 4). A high temperature run is shown in Figure 15. In the OH* emission trace, there is a sudden sharp rise in the signal showing a clear onset of ignition. The pressure trace also shows a sudden instantaneous rise in magnitude giving a precise indicator of ignition.

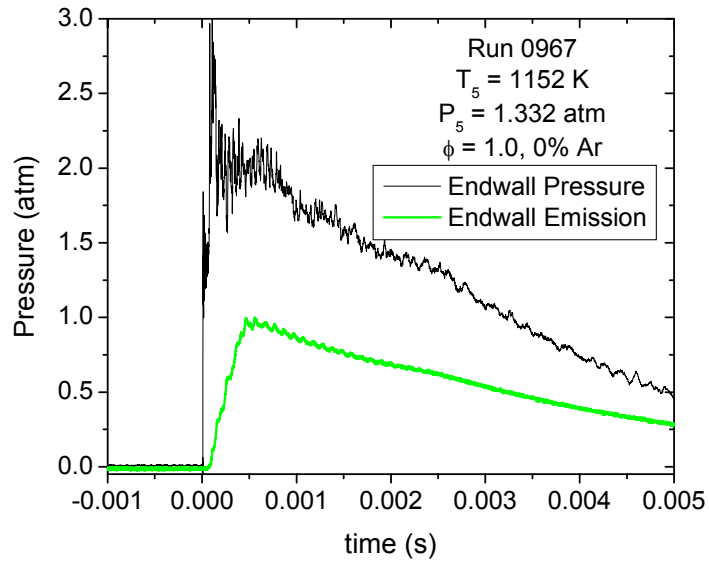


Figure 15: Typical High Temperature Data

Figure 16 shows a low-temperature pressure and emission trace from the same mixture as Figure 15. Both the pressure and emission signals show a gradual rise in magnitude starting at 200 μ s until the steepest increase caused by ignition at 250 μ s

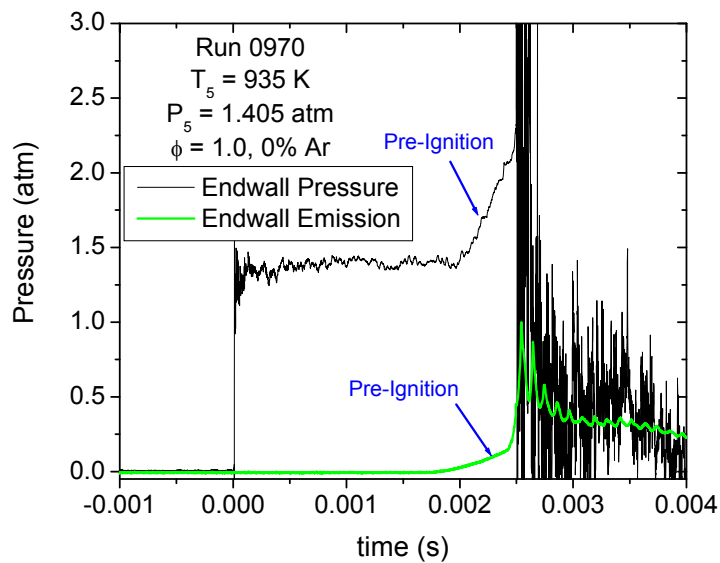


Figure 16: Typical Low Temperature Data Showing Pre-Ignition

The chemical kinetics models do not predict this pre-ignition event. Figure 17 shows the low temperature OH* emission obtained from both the experimental results and the kinetics model. In this figure, the ignition times are synchronized to compare the species profile, therefore ignition times cannot be determined quantitatively based on the time scale shown.

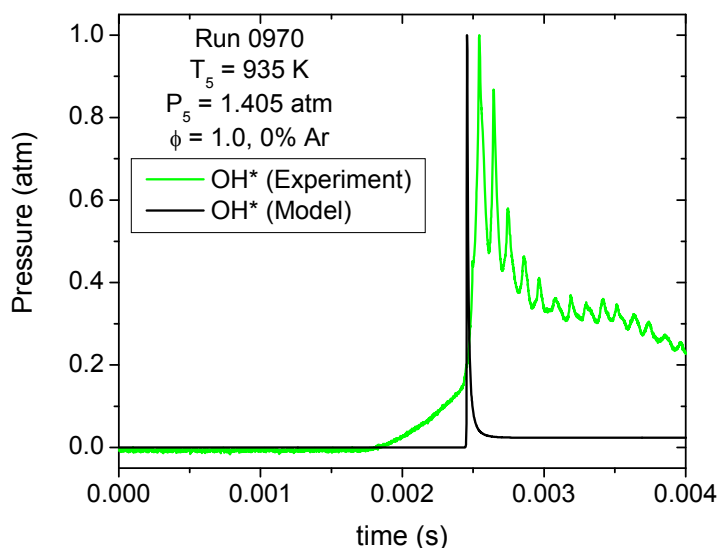


Figure 17: OH* Profile Comparison at Low Temperature

As shown in Figure 17, the model has a sharp rise at ignition and does not show the pre-ignition event. The difference in species profiles between the experiment and the model may explain the large discrepancies between the ignition delay time as determined by the model compared to the experimental data. Pre-ignition generates the additional energy required to cause the remaining test gas to ignite earlier than

expected. With pre-ignition not occurring in the model, this additional energy is not included, and the ignition delay time is much slower than the experimental values.

Pre-ignition at lower temperatures was also noted by Kalitan et al. [2,3] with similar CO/H₂ mixtures over a wide range of test conditions. In the data presented by Kalitan, the measured experimental ignition delay time was faster than the model by a factor of 5. The accelerated ignition delay time was partially attributed to inaccurate rates in the kinetics models, which will be discussed later, but also to pre-ignition. While the cause of pre-ignition was not determined, possible cited causes were detonation effects, heat released by the incident shock wave, and gas impurities [2,3]. Gas impurities were shown to be insignificant due to higher temperature data not showing similar inconsistencies.

Species Profile Comparisons

As previously discussed, the highly dilute mixtures were tested in the shock tube to obtain accurate OH* emission profiles. The dilute mixtures contain less fuel and as a result are less exothermic. The reduction in released energy prevents the optical detection devices from becoming saturated with light emitted from the shock tube. Saturation of the photomultiplier limits the overall light gathered and inaccurately records light emission after ignition.

While the reduced emission magnitude increases the accuracy of the photomultiplier tube, it also causes a decrease in the signal-to-noise ratio. This signal-to-noise ratio starts to become an issue for the coldest shock tube runs with low light emission. An example of emission data gathered with low signal-to-noise ratio is shown in Figure 18.

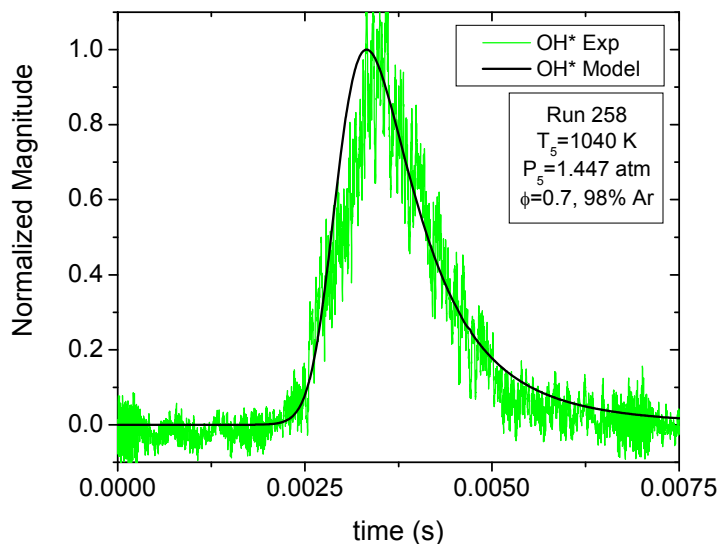


Figure 18: Emission Data with Low Signal-to-Noise Ratio

These species profiles of OH* can be used to study the time response with respect to the magnitude of the signal [16]. Since OH* is an indicator of the reaction, its time history can provide information about the magnitude and duration of the combustion reaction [9]. This history when compared to the chemical kinetics model is then used to validate or provide data to improve the mechanism.

The OH* profiles were obtained for each shock tube run, and were then compared to the kinetics model with matching temperature and pressure conditions. The species

comparisons are provided in Appendix G with a few provided in this chapter for discussion.

Most runs showed accurate predictions of OH* at the onset of ignition through the peak emission. The slope of the ignition event matches the model extremely well in most cases as shown in Figure 19. This shows that despite the significant differences in measured ignition delay times, the model does accurately predict the reaction rates during ignition.

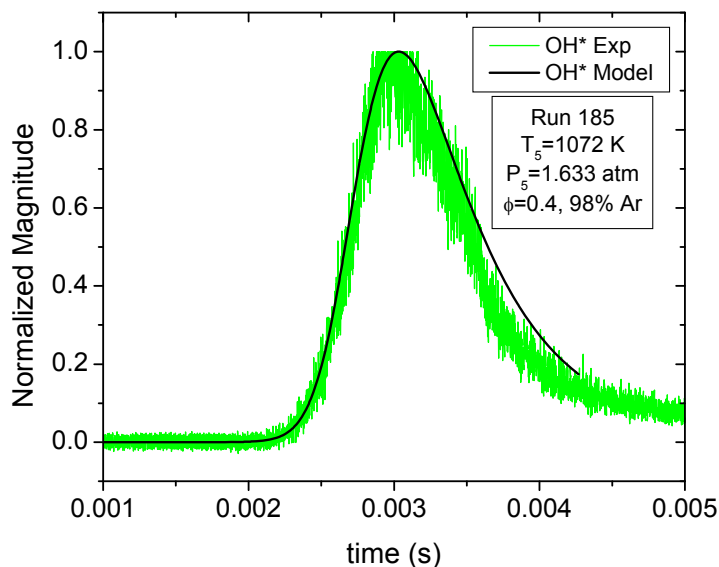


Figure 19: OH* Species Comparison with Good Agreement

The decrease in emission was much slower in the model compared to the measured emission for most cases. The model predicts a much more gradual decrease in emission, and consequently the overall reaction, lagging the measured emission trace by approximately 1 ms. This trend is more evident in the higher-temperature traces.

Figure 20 shows a significant difference in the trace after the peak emission, where the temperature behind the reflected shock was 1437 K, compared to the low-temperature species profile at 1072 K previously shown in Figure 19.

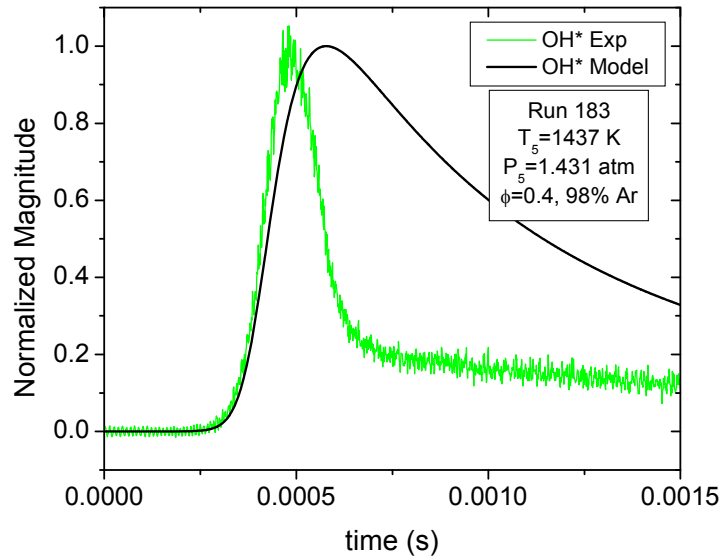


Figure 20: OH* Species Comparison with Poor Agreement

Figure 20 also shows a residual emission behind the main ignition event with a magnitude of approximately 20% of the peak emission. The model has a gradual fall and does not show this change in slope after the peak. This may be due to reflected light emission from other sections of the shock tube other than the position at the observation window.

With respect to equivalence ratio, the species profiles of OH* were in better agreement with the stoichiometric mixture ($\Phi=1.0$) compared to fuel lean mixtures ($\Phi=0.7$ and $\Phi=0.4$). While most data show poor agreement with the emission trace after the peak,

the fuel lean mixtures showed further disagreement with the initial rise of the emission compared to the stoichiometric mixture. This discrepancy between the data and the model is further exaggerated at high temperatures (above 1100 K).

The species profile comparisons were performed with normalized magnitudes. For comparison of the overall magnitude of the measured vs. predicted emission, calibration of the measured OH* emission could be performed using well known and accepted mixtures [15]. Once calibrated, the profile comparisons may show significant differences in the peak emission values, and provide additional data for model improvement. Such calibrated OH* measurement were beyond the scope of the present thesis.

Data Comparison to Other Work

Similar data have been obtained by Kalitan et al. [3] for a wide range of CO/H₂ mixtures. That work used a real syngas mixture with approximately 5/95% CO/H₂ and several other constituents included and an average pressure of 1.7 atm. The most-similar data obtained by Kalitan contained only CO/H₂ with a ratio of 20/80% and an average pressure of 1.1 atm.

While there are several differences, a direct comparison shows that the data are in general agreement as shown in Figure 21. While there is a slight difference in pressure between the two experiments, the primary difference is the concentration of H₂ in the

fuel mixture. The difference in slope between the two experiments can be attributed to the difference in H₂ concentration. Increased H₂ concentration causes the change in slope to occur at a lower temperature [2]. This difference in slope is evident in Figure 21 and agrees with the expected behavior relative to H₂.

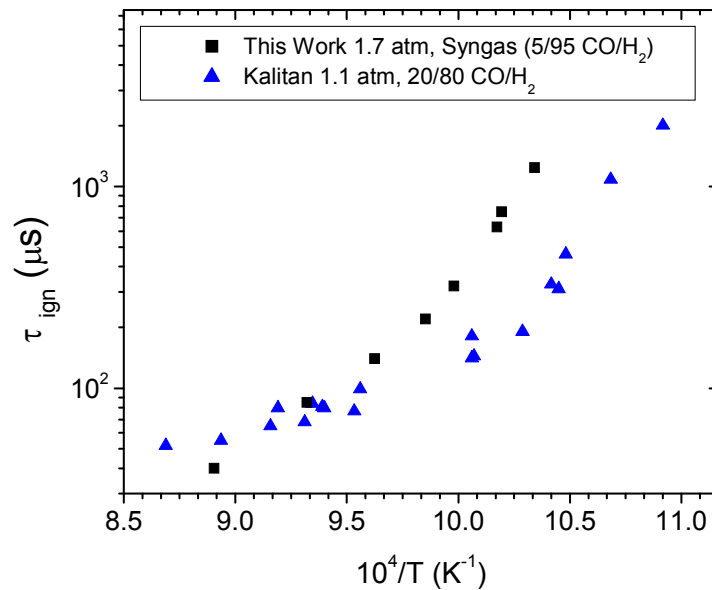


Figure 21: Comparison to Other Syngas Data of Similar Pressure

Both this work and the experiments run by Kalitan have similar results, with fairly good agreement with the model at high temperatures, and poorer agreement at lower temperatures. Kalitan also noted the presence of pre-ignition at lower temperatures [3].

Kalitan [3] also performed sensitivity analysis with the kinetics models and syngas fuels. The purpose was to determine reactions which have the largest effect on ignition delay time, which would be candidates for modification in order to improve model

performance. It was the conclusion that the CO₂-forming reactions, CO + O + M and CO + HO₂, significantly slow ignition in the model at lower temperatures, and require improvement for accurate model predictions [3]. However, the magnitude of the discrepancy may be too large for mechanism reaction rate modifications alone [5].

CONCLUSIONS

The increasing use of syngas in power generation turbines has created a need for ignition data to understand and optimize the fuel combustion process. Initial syngas data have shown significant disagreement with modern chemical kinetics models which were considered to be accurate and understood [2,3,5,6]. To supplement these data and attempt to provide additional insight, a specific syngas mixture of commercial importance was tested behind reflected shock waves in a shock tube. Ignition delay time and emission profiles were obtained from the experimental data for equivalence ratios of 0.4, 0.7, 1.0, and 2.0, with temperatures ranging from 913 K to 1803 K, at atmospheric pressure. The experimental data were compared to a chemical kinetics model using the Davis et al. [7] mechanism.

The model had relatively good agreement with the experimental ignition delay time data at temperatures above 1000 K. The low temperature data were in disagreement with the model, but agreed with results obtained during similar experiments by other researchers [2,3,5,6]. The similarities with this work and that of other researchers shows the model over predicting ignition delay time by more than an order of magnitude at the lowest temperatures.

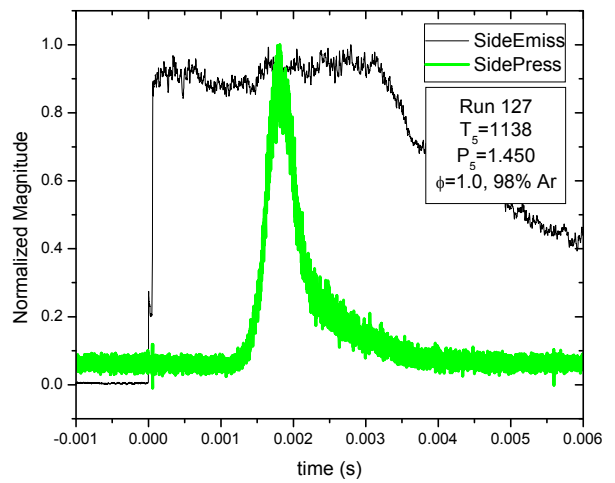
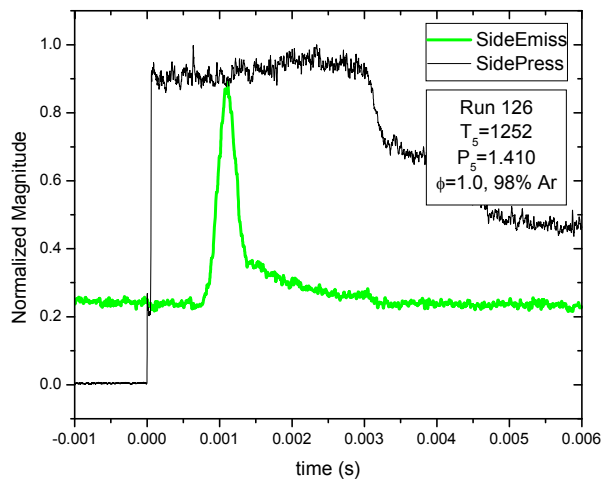
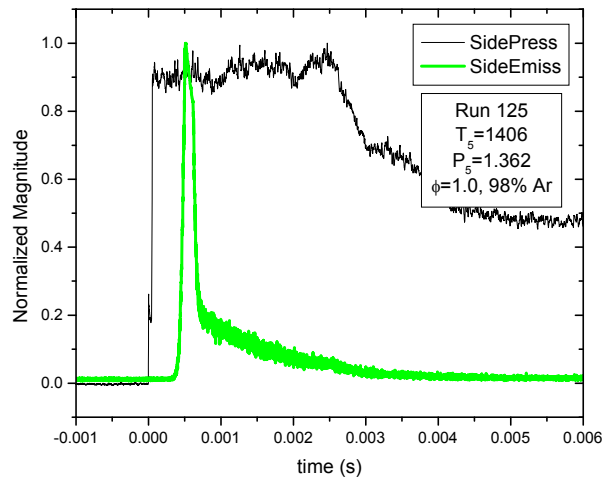
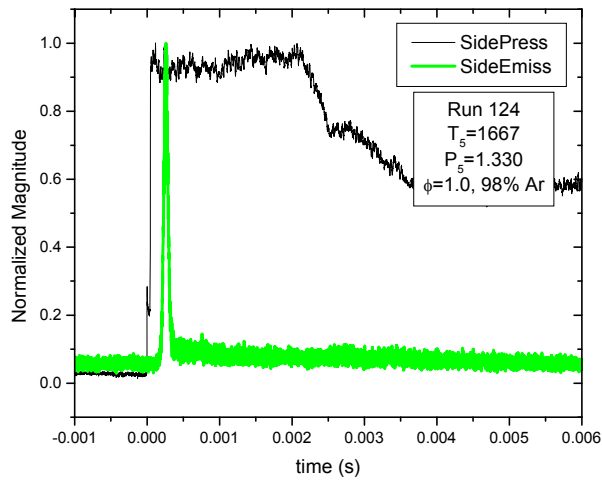
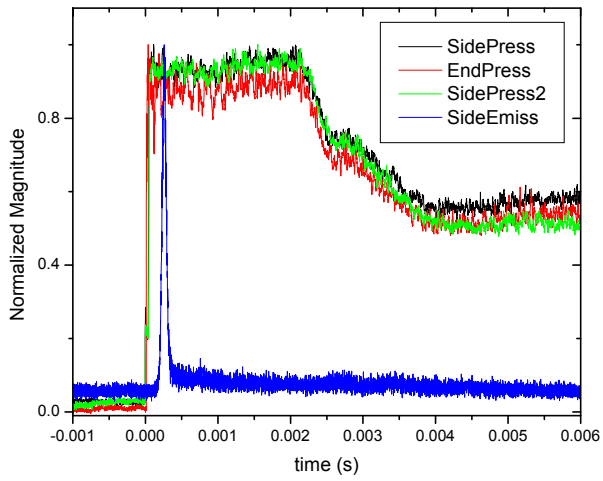
Species profile analysis of the OH* emission showed good agreement in most cases but a significant difference in the formation and/or depletion rates of OH* was seen in some of the data. Since the use of OH* is a well established method for ignition diagnostics

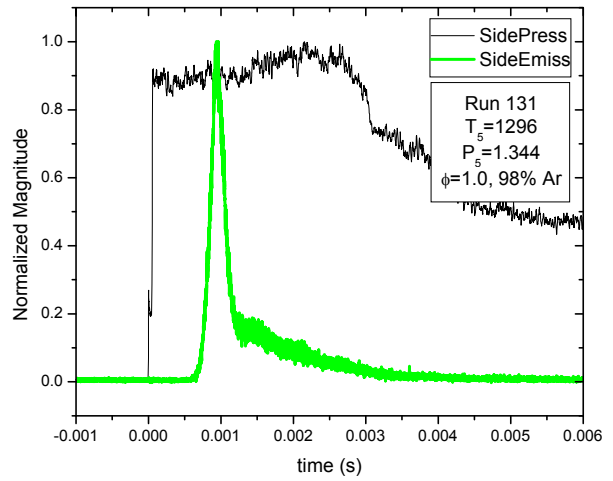
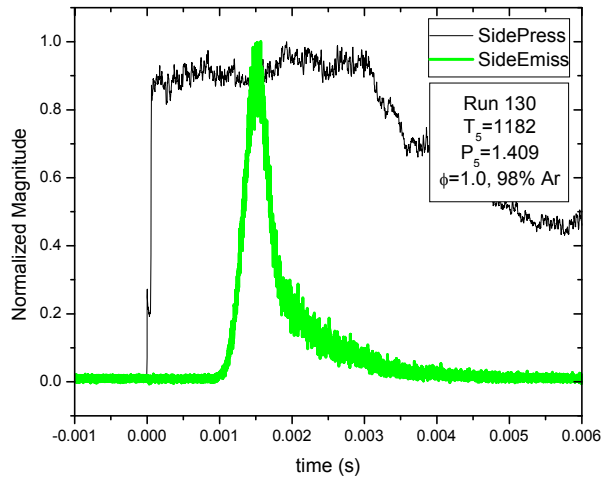
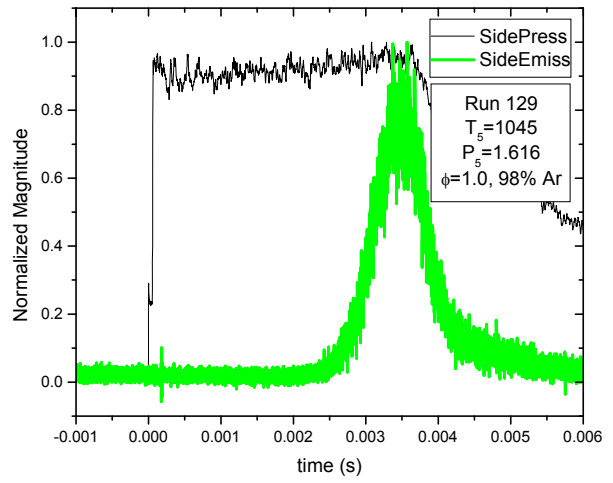
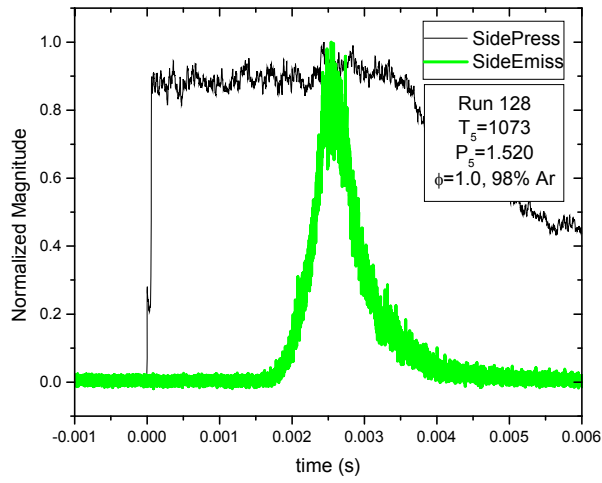
[21], the error is likely in the kinetics in which the reaction path and rates are not well understood for these mixtures. The kinetics are considered well understood for several of the syngas constituents individually, however this performance cannot be used to assume accuracy of the combined mixture [19].

Pressure and emission profiles showed a pre-ignition rise in both signals prior to the main ignition event in the lowest-temperature runs. Pre-ignition was not evident in the kinetics models which may explain the difference in ignition delay time. Understanding of the cause of the pre-ignition reactions causing a rise in pressure and emission must be understood to further improve the ability to predict combustion characteristics of syngas using the chemical kinetics models.

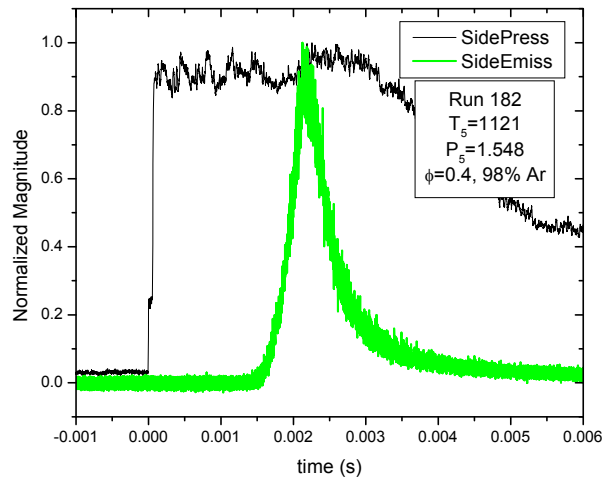
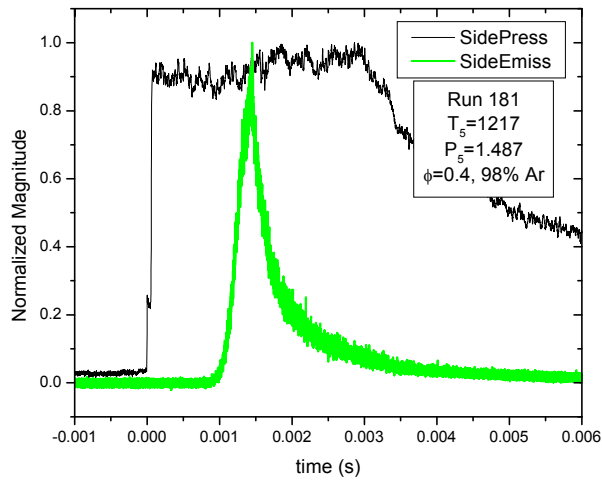
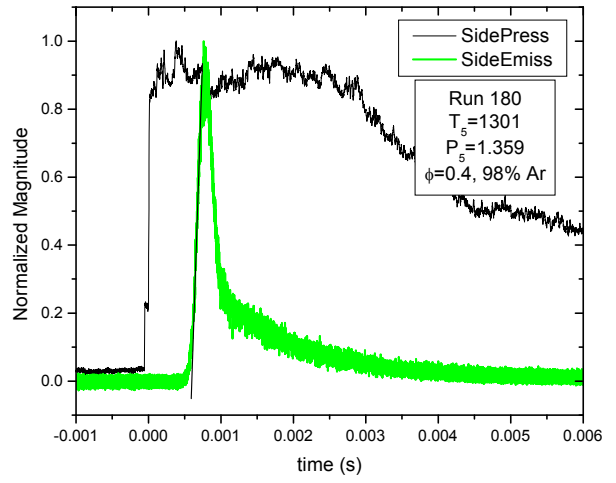
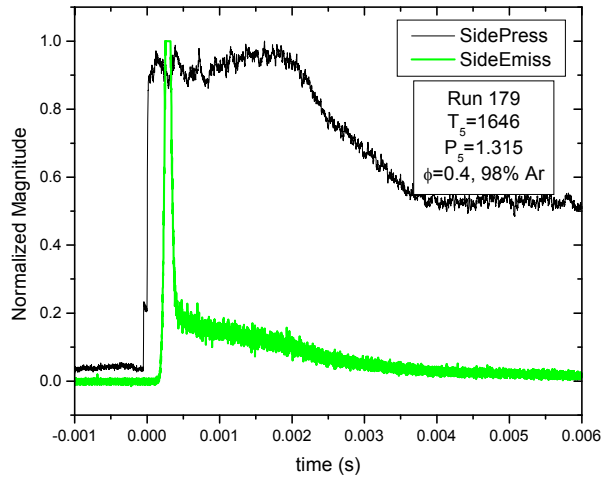
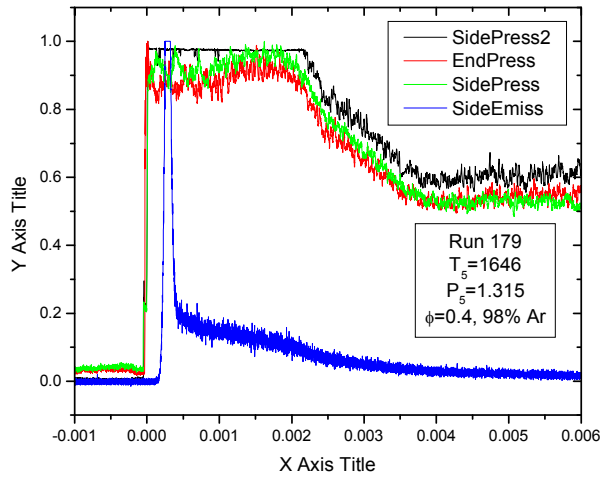
The data presented herein support recent findings and further express the need to better understand the chemical kinetics of syngas mixtures. The species profiles show the mechanism does not accurately predict the ignition and quenching rates at all conditions, which suggests improvements to the mechanism are required for accurate prediction of syngas properties. A broad review of the data suggests the model discrepancies may be too large for mechanism reaction rate modifications alone [5]. Further research is required to improve chemical kinetics models with respect to syngas and other CO/H₂ mixtures.

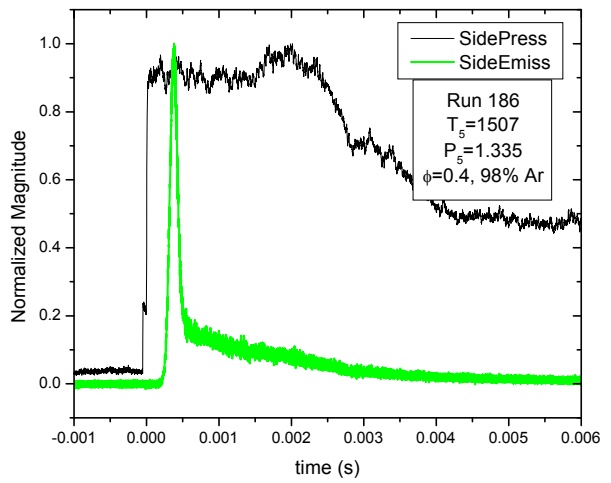
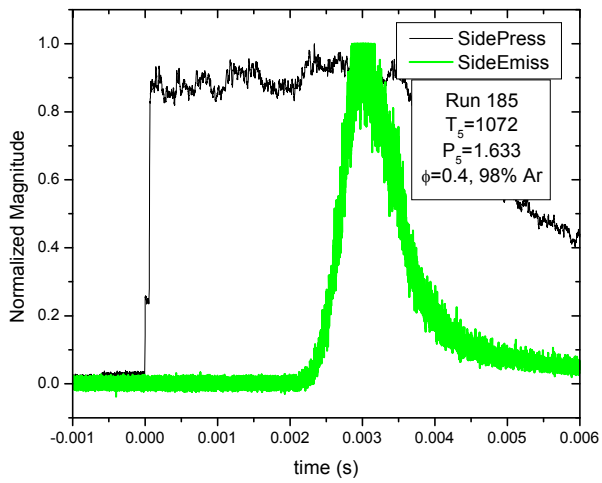
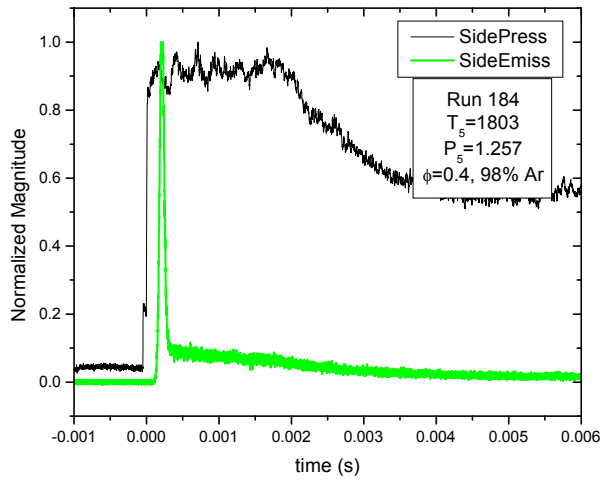
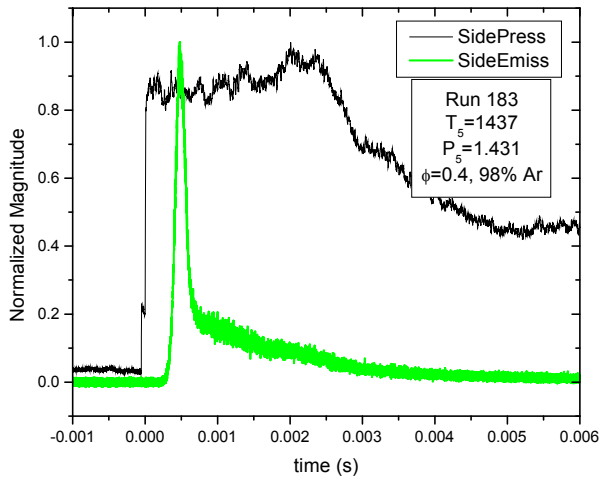
APPENDIX A: MIX 19 RUN DATA



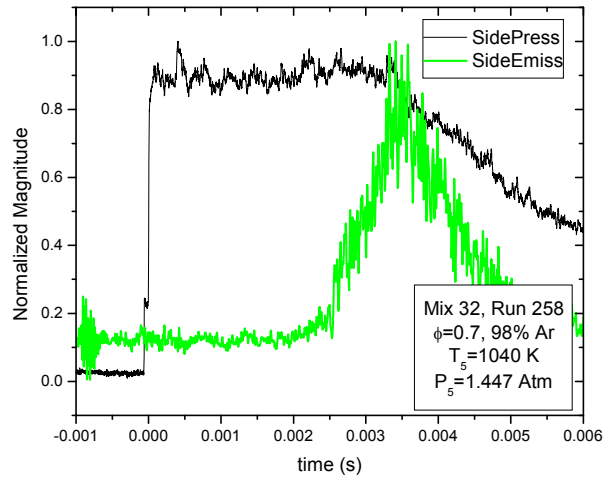
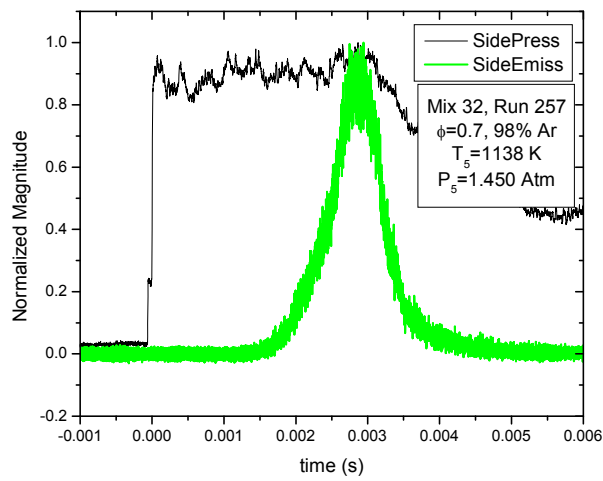
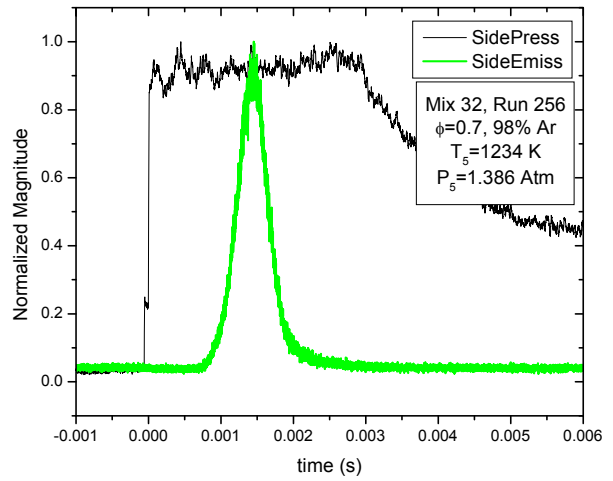
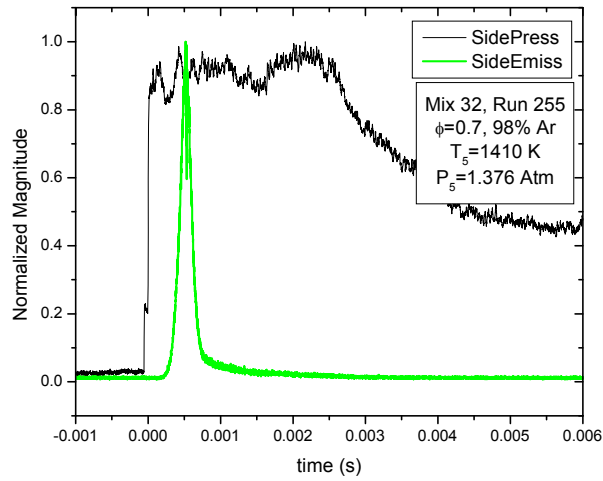
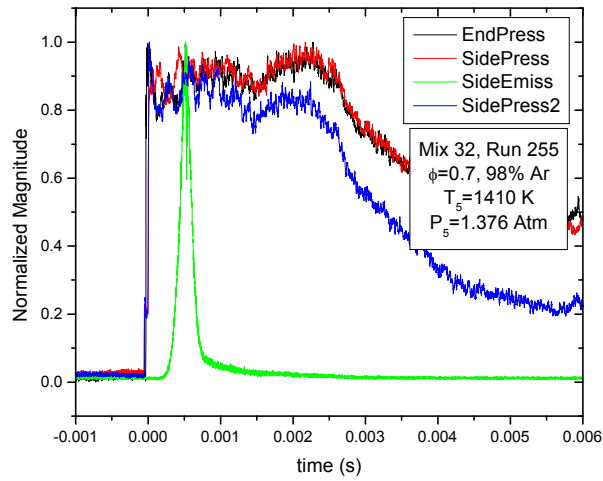


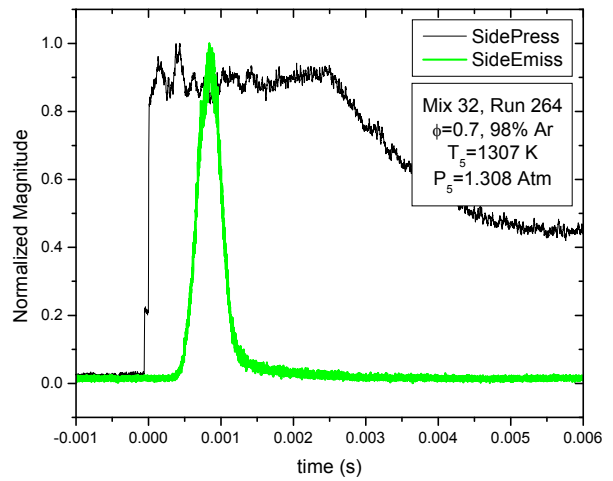
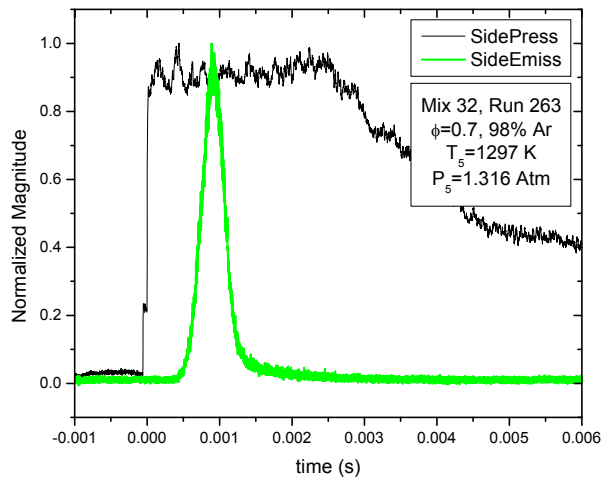
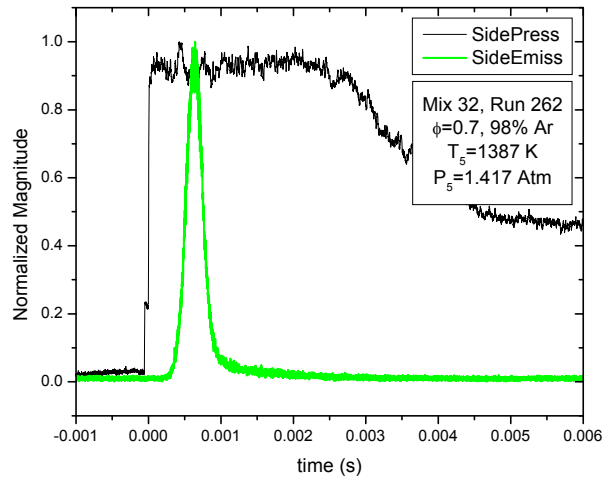
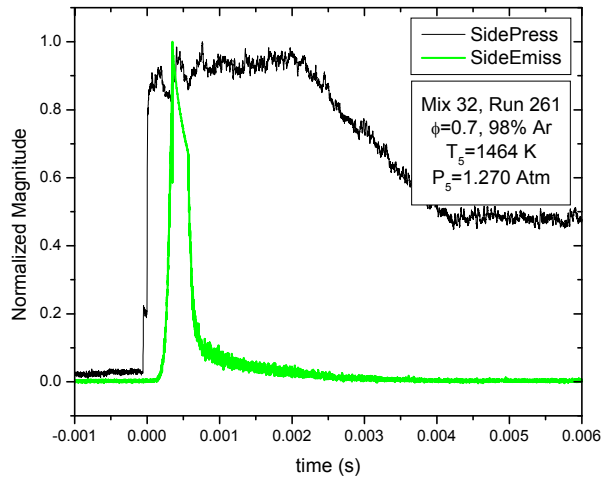
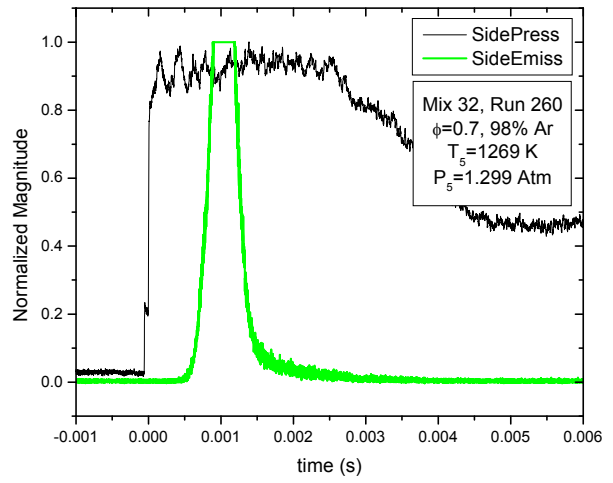
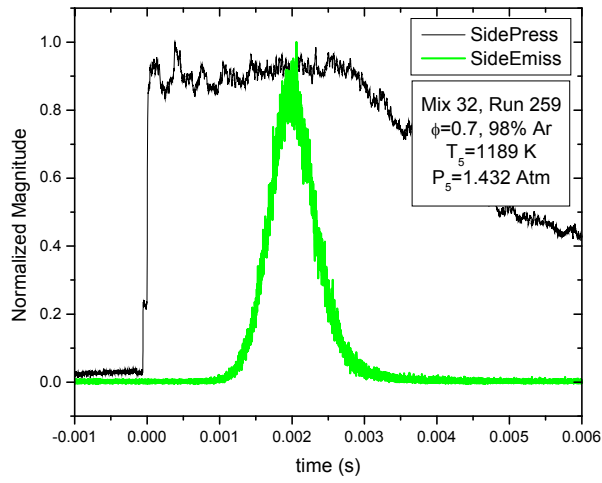
APPENDIX B: MIX 25 RUN DATA



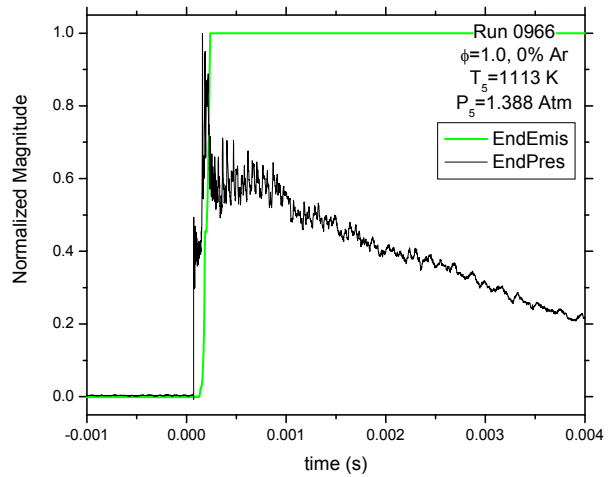
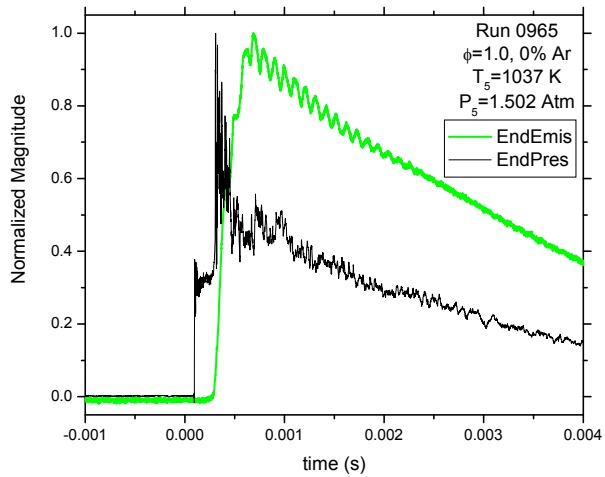
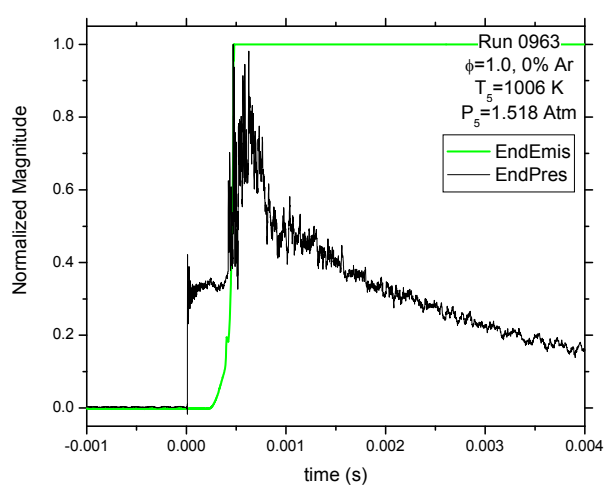
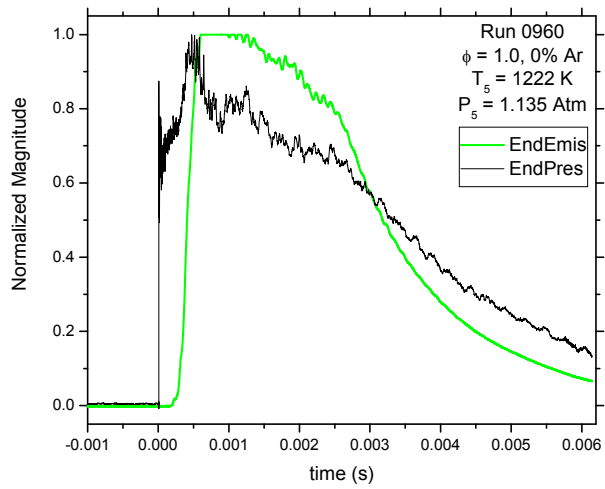
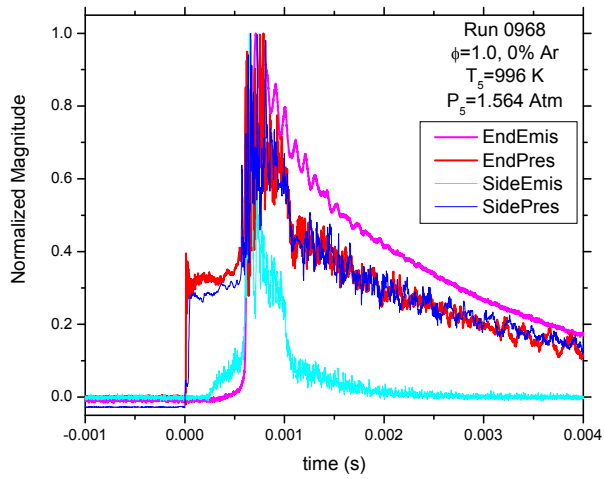


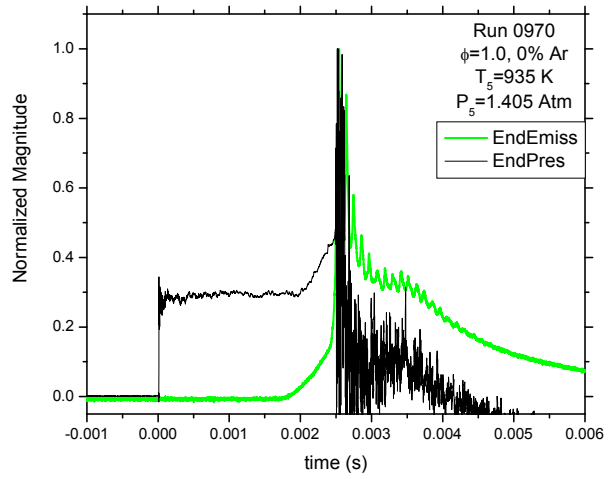
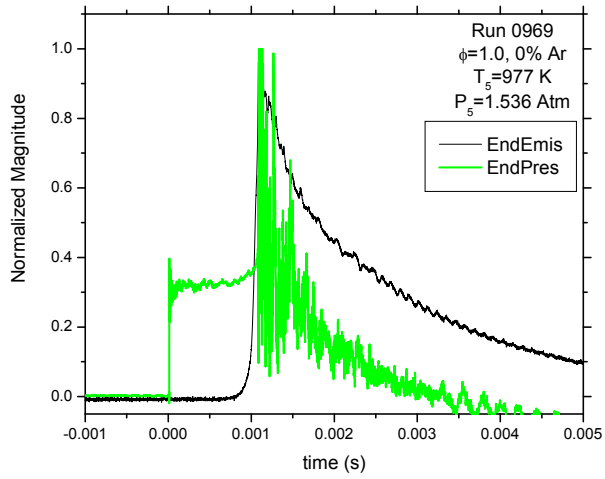
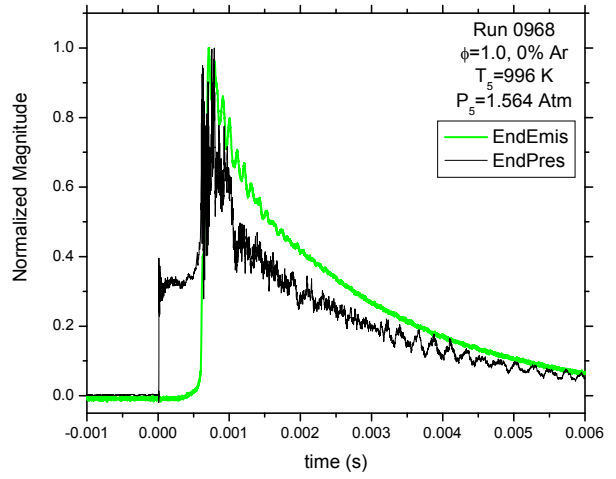
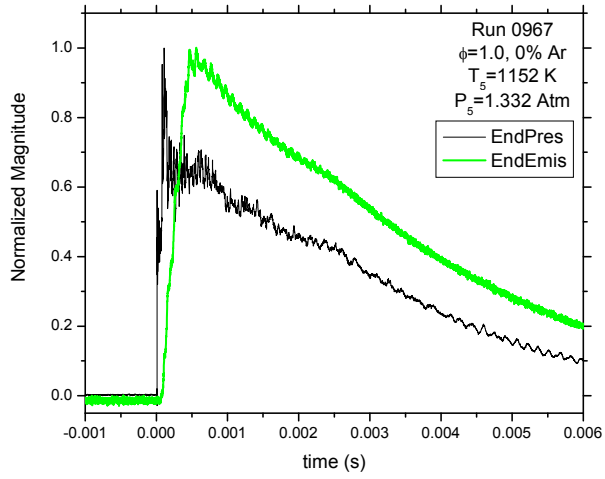
APPENDIX C: MIX 32 RUN DATA



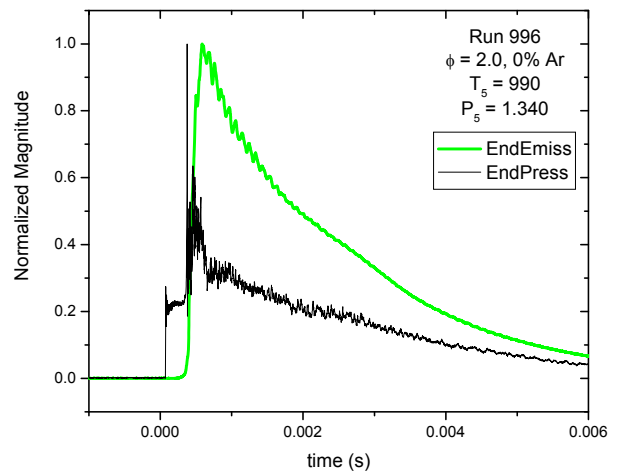
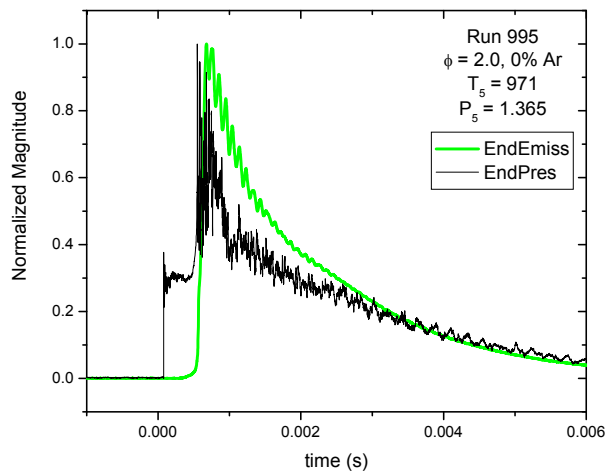
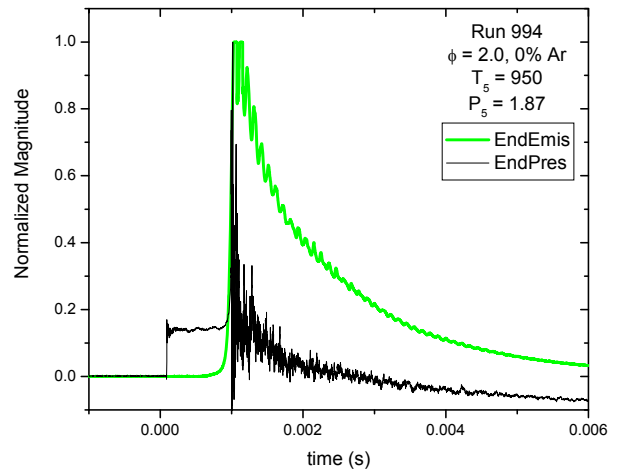
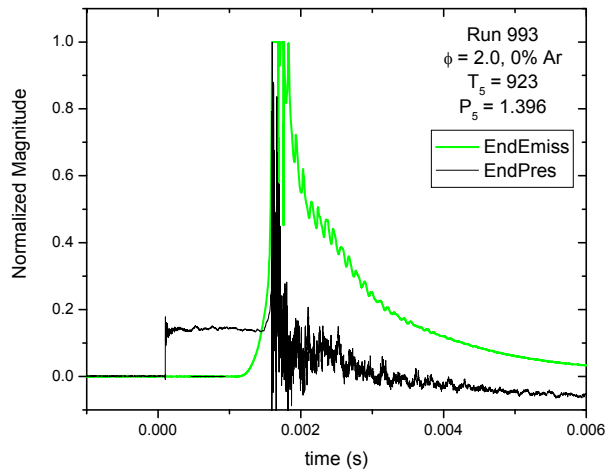
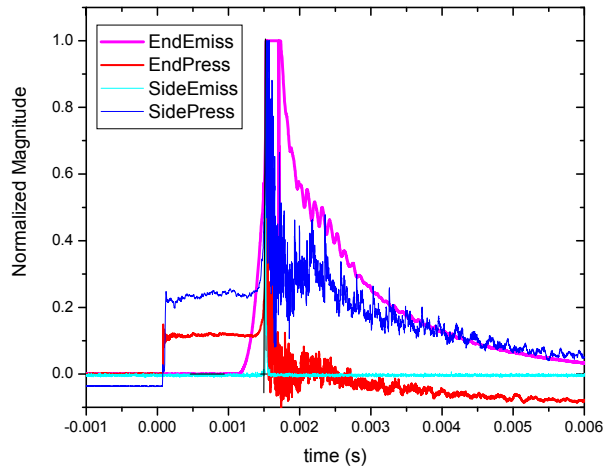


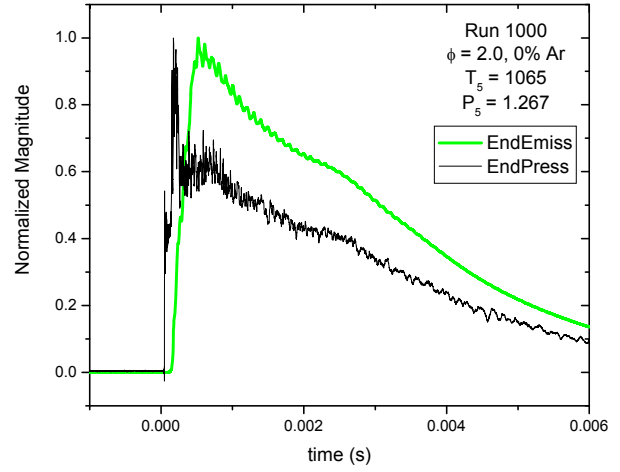
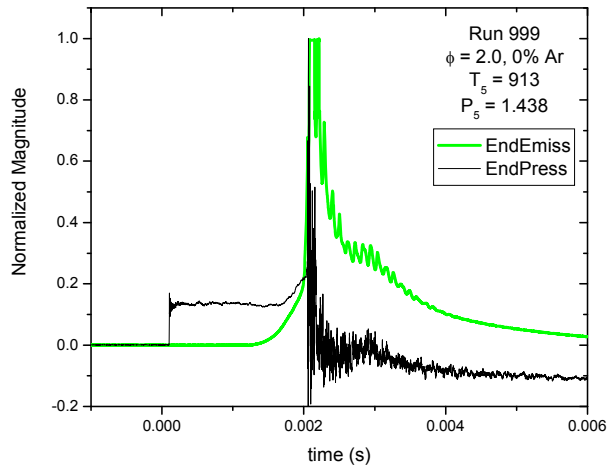
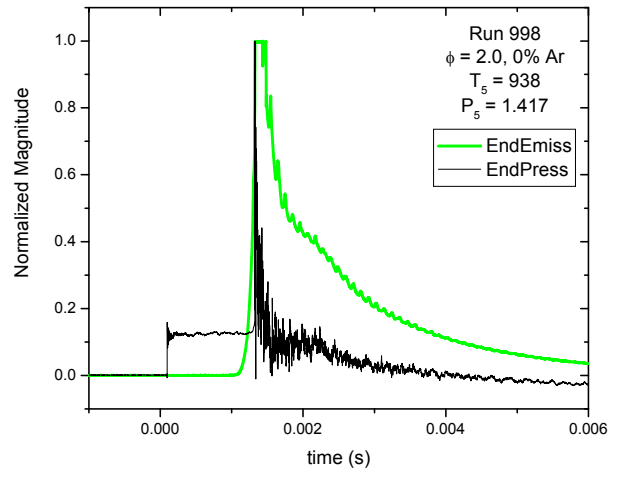
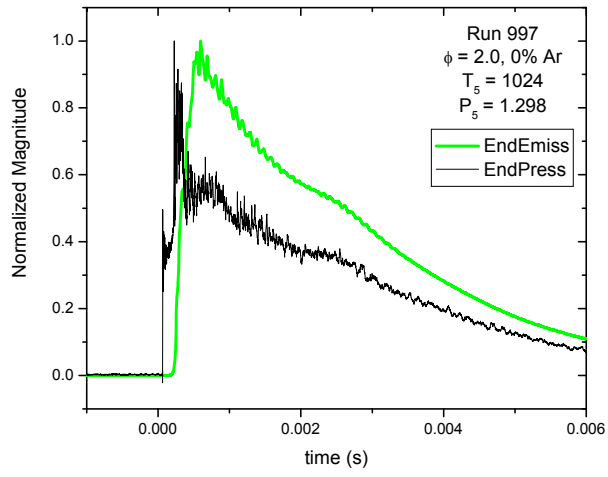
APPENDIX D: MIX 83 RUN DATA



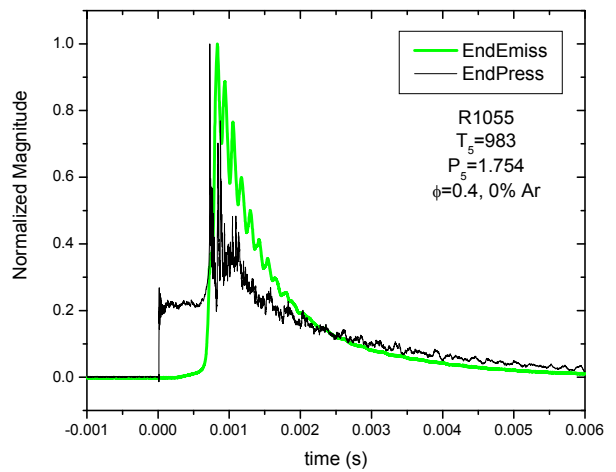
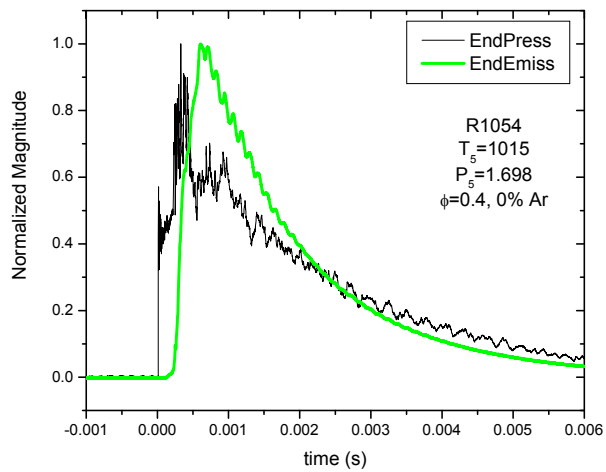
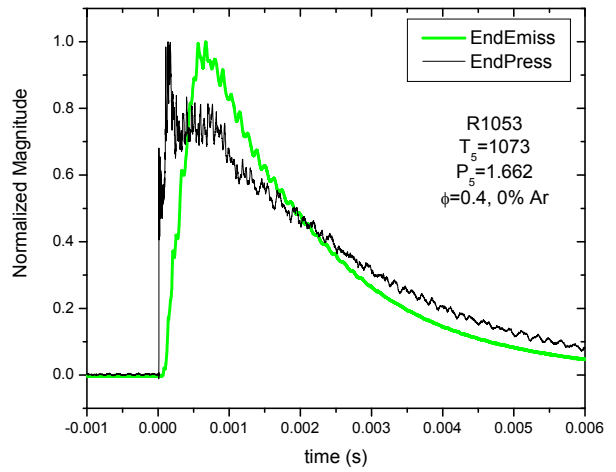
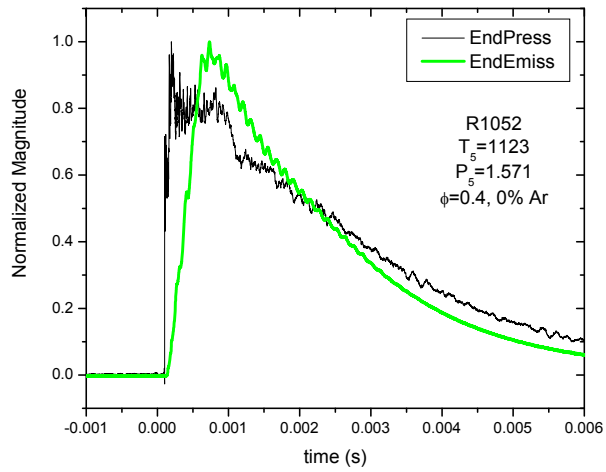
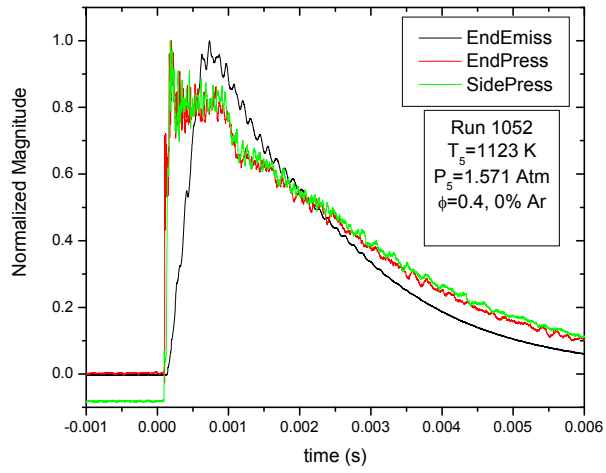


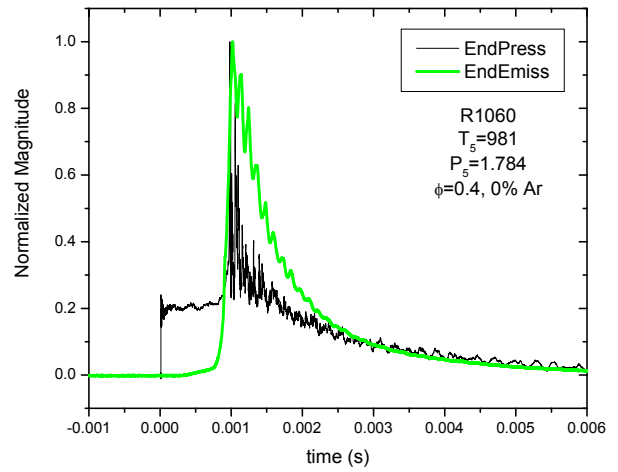
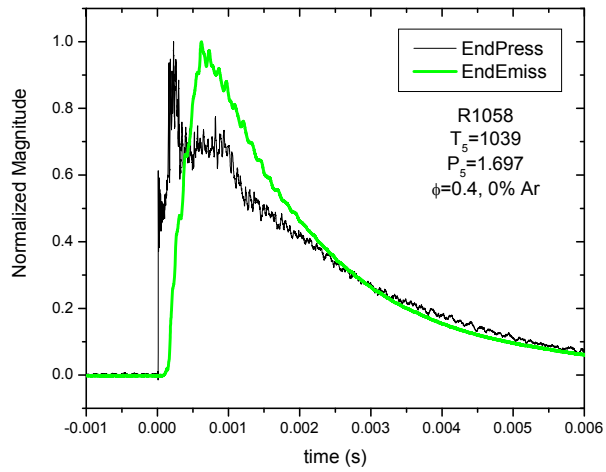
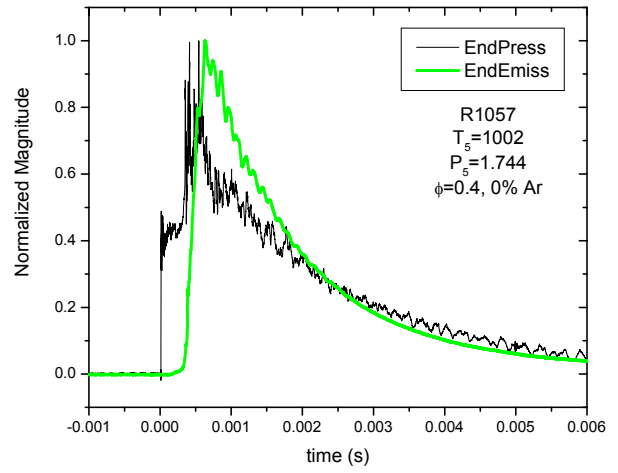
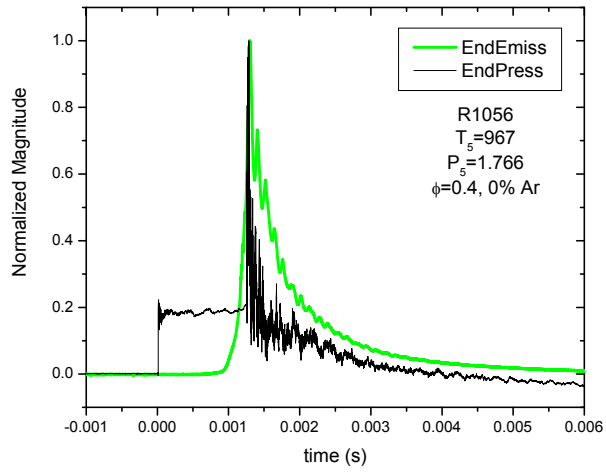
APPENDIX E: MIX 87 RUN DATA





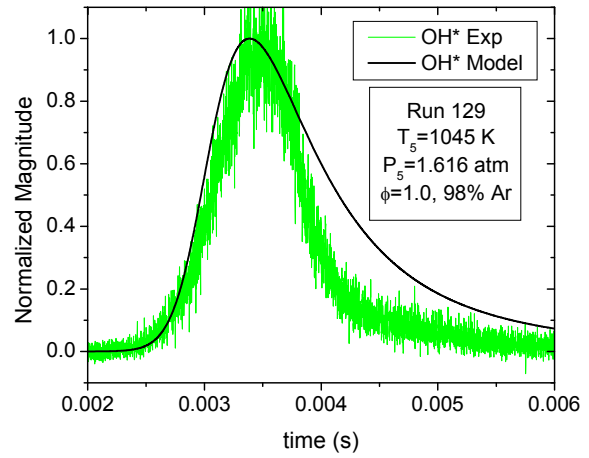
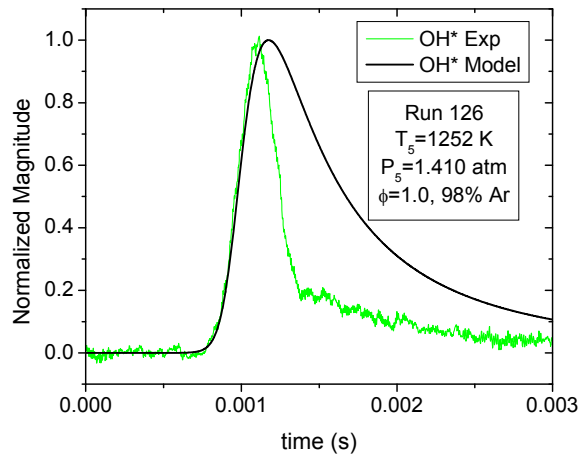
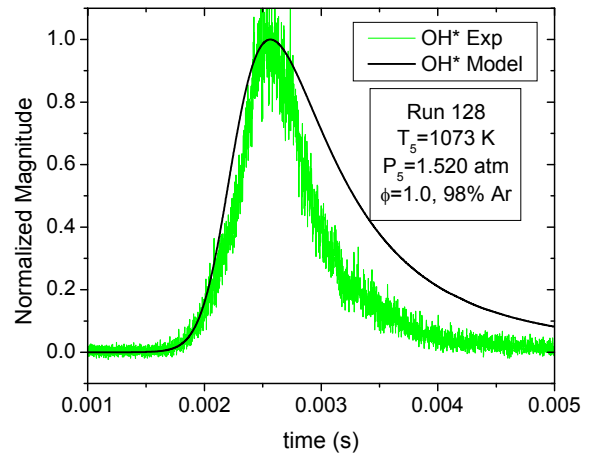
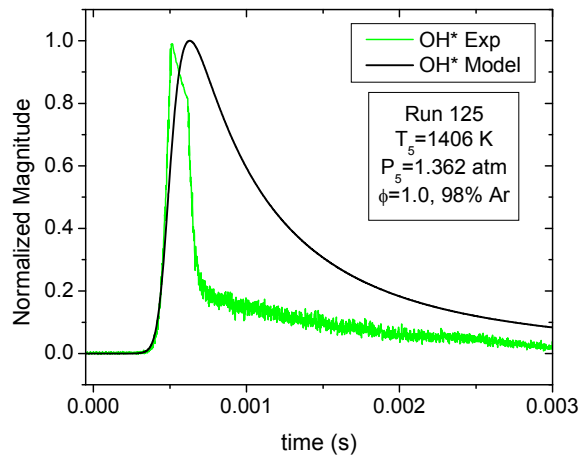
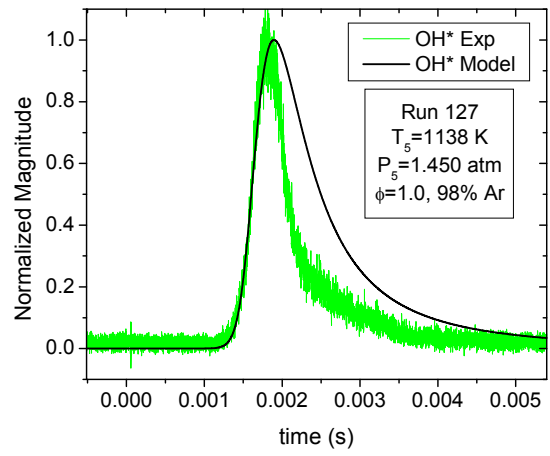
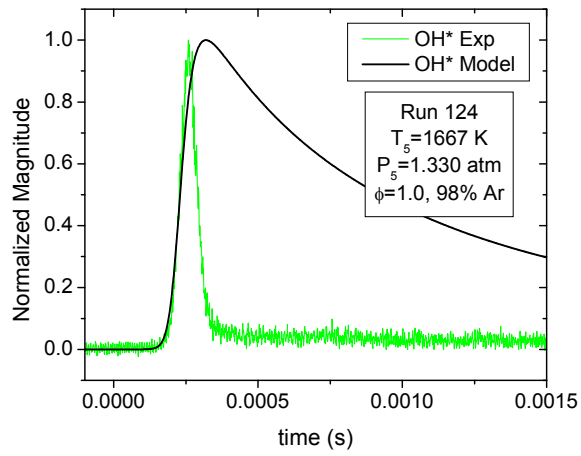
APPENDIX F: MIX 90 RUN DATA

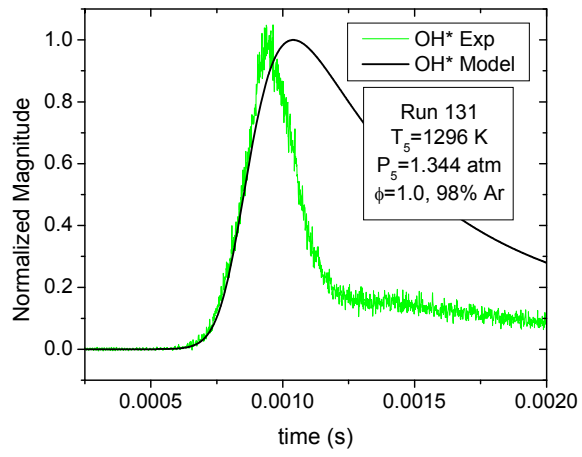
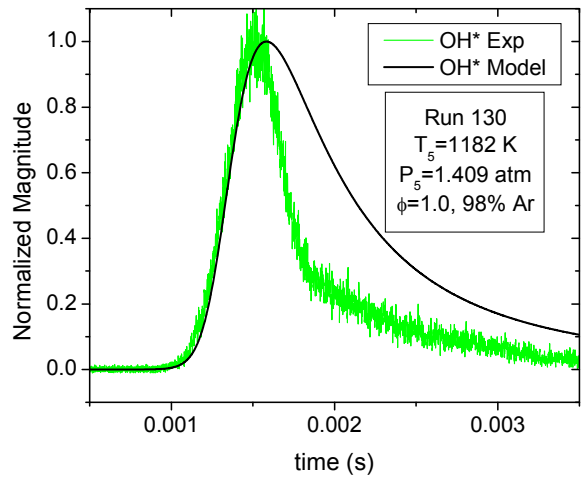




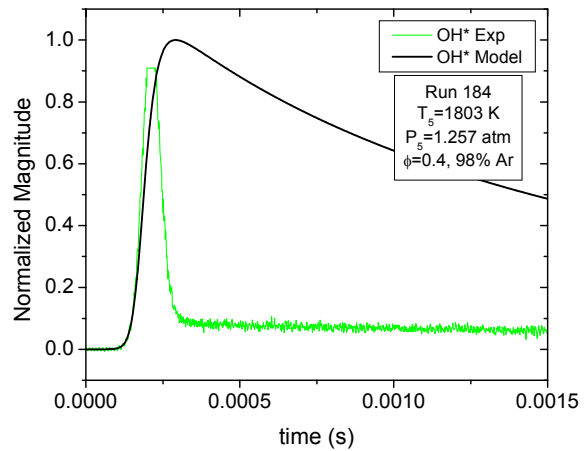
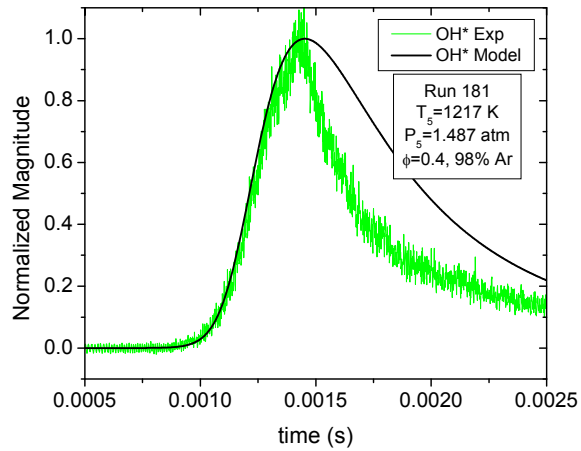
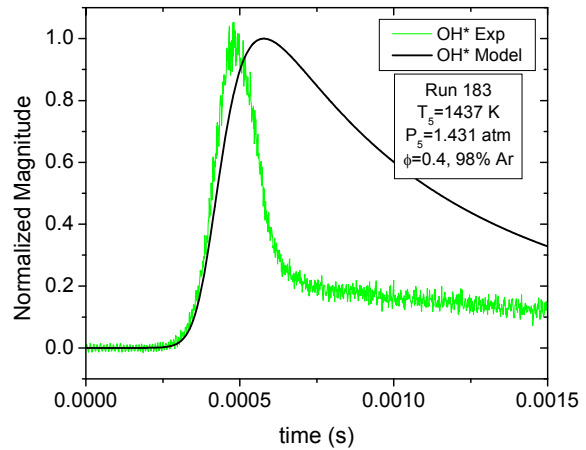
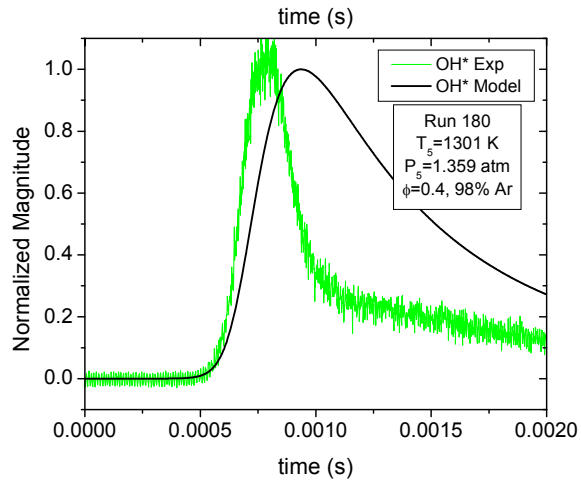
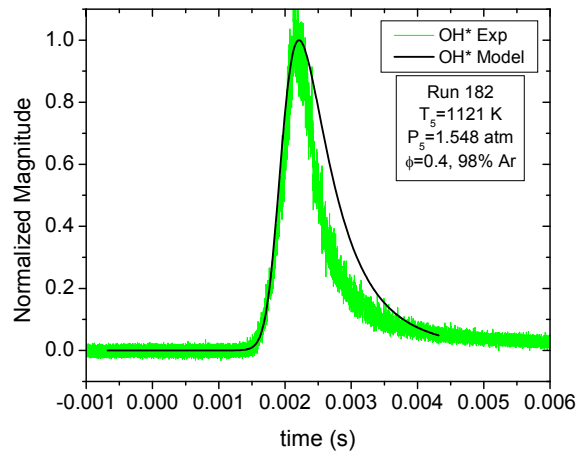
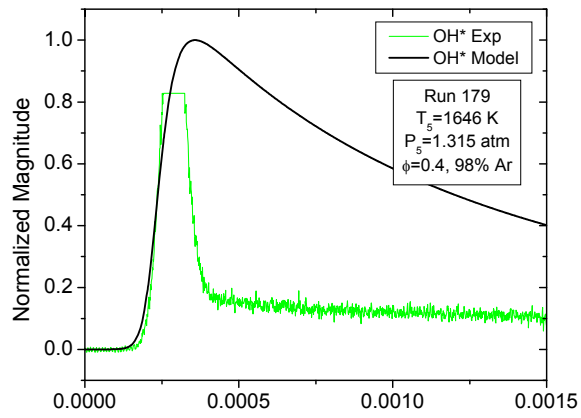
APPENDIX G: SPECIES PROFILE COMPARISON

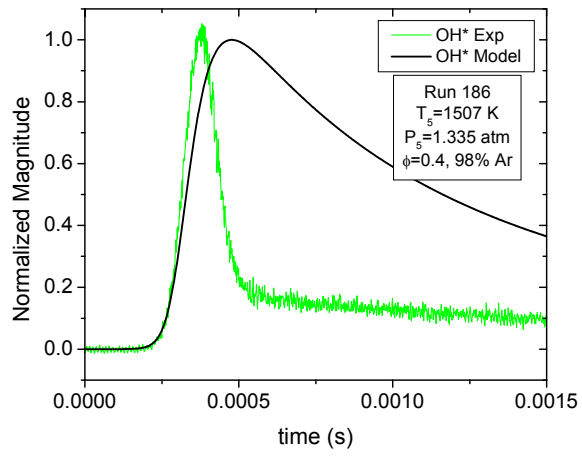
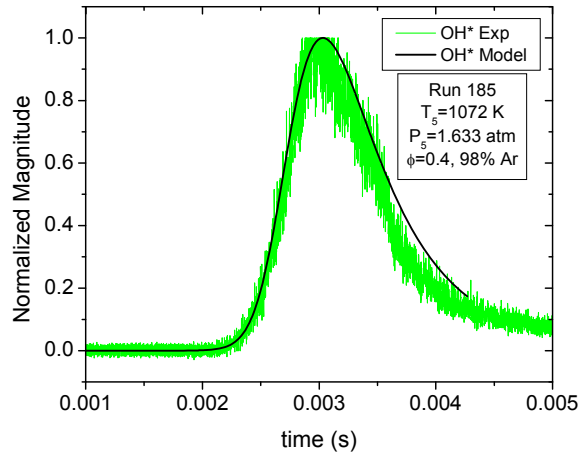
Mixture 19



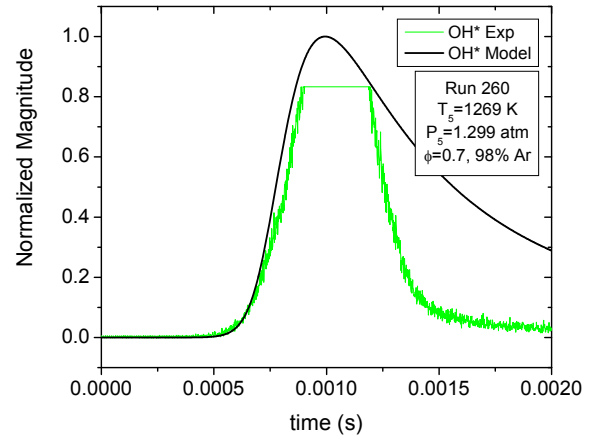
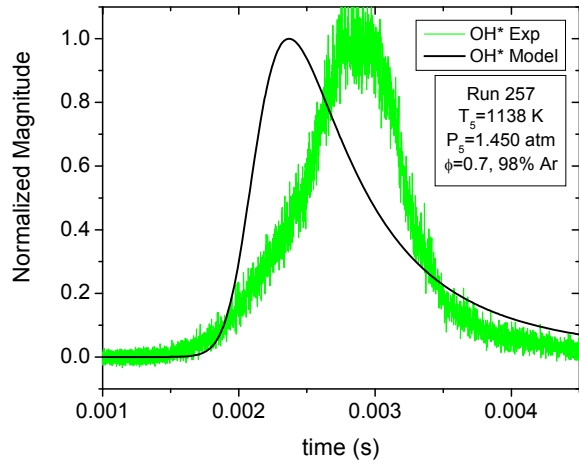
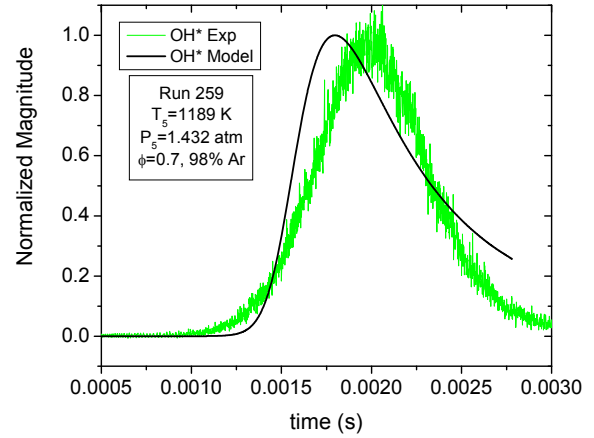
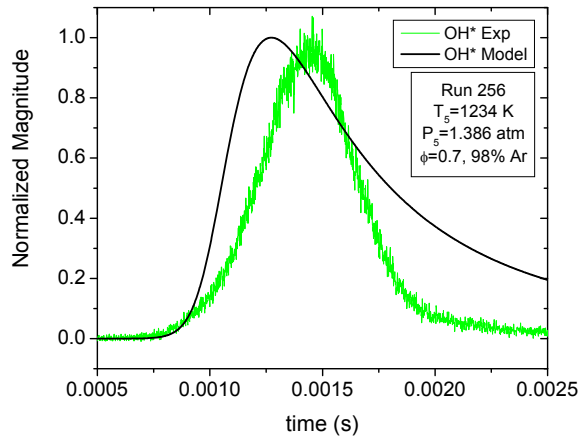
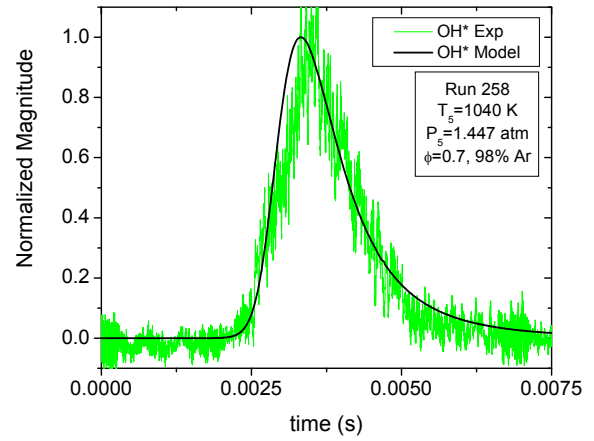
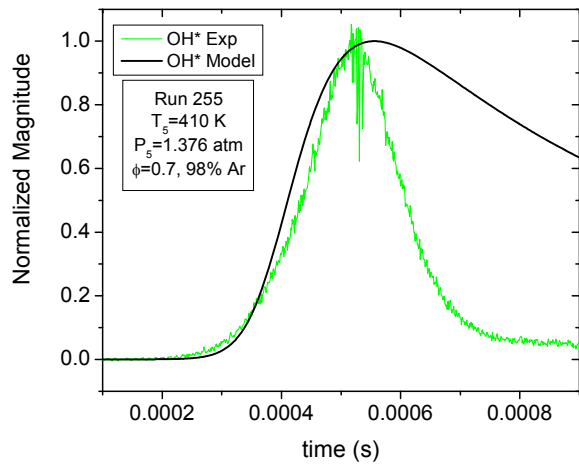


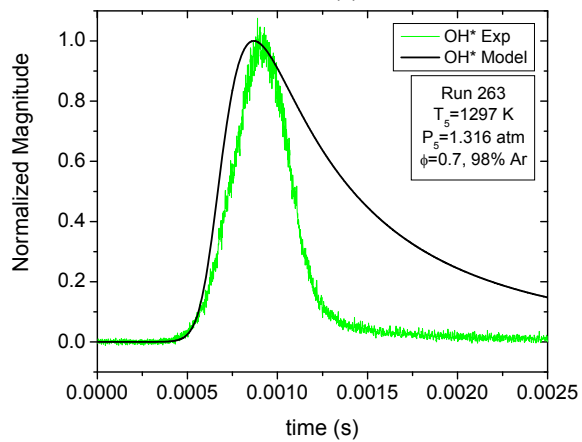
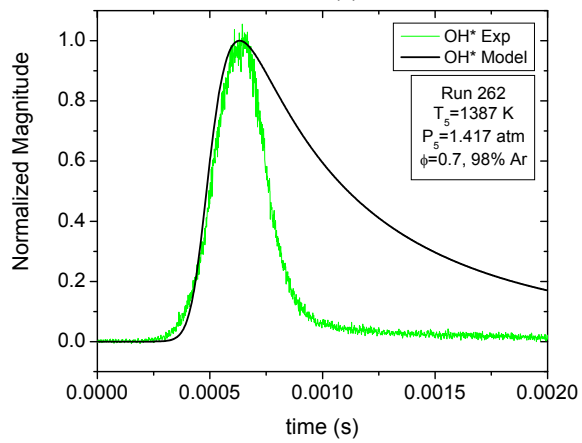
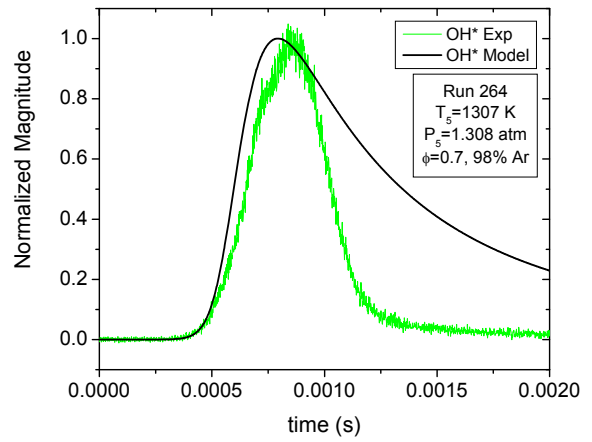
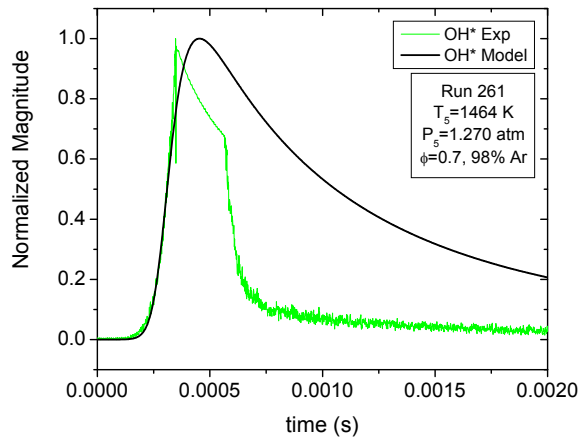
Mixture 25





Mixture 32





LIST OF REFERENCES

1. G.A. Richards, M.M. McMillian, R.S. Grimmens, W. A. Rogers, and S. R. Cully, "Issues for Low-Emission, Fuel-Flexible Power Systems," *Progress in Energy and Combustion Science*, Vol. 27, pp. 141-169, 2001.
2. D.M. Kalitan and E.L. Petersen, "Ignition and Oxidation of Lean CO/H₂ Fuel Blends in Air," *AIAA 2005-3767*, 41st AIAA/ASME/SAE/ASEE Joint Propulsion Conference and Exhibit, Tucson, Arizona, July 10-13, 2005.
3. D.M. Kalitan and E.L. Petersen, "Ignition of Lean CO/H₂/Air Mixtures at Elevated Pressures," GT2006-90488, *Proceedings from ASME Turbo Expo*, Barcelona, Spain, June 6-9, 2006.
4. J. Crook, "Back to the future", *IET Power Engineer*, June/July 2006, pp. 26-29.
5. E.L. Petersen, D.M. Kalitan, A.B. Barrett, S.C. Reehal, J.D. Mertens, D.J. Beerer, R.L. Hack and V.G. McDonell, "New Syngas/Air Ignition Data at Lower Temperature and Elevated Pressure and Comparison to Current Kinetics Models," *Combustion and Flame*, 149 (1-2), pp. 244-247, 2007.
6. S.C. Reehal, D.M. Kalitan, T.J. Hair, A.B. Barrett and E.L. Petersen, "Ignition Delay Time Measurements of Synthesis Gas Mixtures at Engine Pressures," *Proceedings from the Western States Section of the Combustion Institute 5th US Combustion Spring 2007 Meeting*, University of California San Diego, March 25-25, 2007.
7. S.G. Davis, A.V. Joshi, H. Wang, F. Egolfsoolous, "An Optimized Kinetic Model of H₂/CO Combustion," *Proceedings of the Combustion Institute*, Vol. 30, pp. 1283-1292, 2005.
8. A.G. Gaydon and I.R. Hurlle, *The Shock Tube in High-Temperature Chemical Physics*, New York, Reinhold, 1963.
9. J.M. Hall, and E.L. Petersen, "Kinetics of OH Chemiluminescence in the Presence of Hydrocarbons," AIAA 2004-4164, *AIAA/ASME/SAE/ASEE Joint Propulsion Conference and Exhibit*, Fort Lauderdale, FL, July 11-14, 2004.
10. R.J. Kee., F.M. Rupley, J.A. Miller, M.E. Coltrin, J.F. Grcar, E. Meeks, H.K. Moffat, A.E. Lutz, G. Dixon-Lewis, M.D. Smooke, J. Warnatz, G.H. Evans, R.S. Larson, C. Wang, and O. Adigun, *Chemkin Collection*, Release 3.6 , Reaction Design, Inc., San Diego, CA, 2000.
11. E. Gonzalez, E.L. Petersen, "The Use of Frosh in Shock-Related Studies and Sandia Thermodynamic Database," White Paper, December 3, 2007.

12. R.J. Kee, F.M. Rupley, and J.A. Miller, "The Chemkin Thermodynamic Database," SAND87-8215B, Sandia National Laboratory, March 1990.
13. GRI-Mech, Software Package, Ver. 3.0, University of California, Berkeley, Berkeley, CA, available at <http://www.me.berkeley.edu/gri-mech/>.
14. M.A. Mueller, R.A. Yetter, and F.L. Dryer, "Flow Reactor Studies and Kinetic Modeling of the H₂/O₂/NO_x and CO/H₂O/O₂/NO_x Reactions," *International Journal of Chemical Kinetics*, Vol. 31, No. 10, pp. 705-724, 1999.
15. E.L. Petersen and D.M. Kalitan, "Calibration and Chemical Kinetics Modeling of an OH Chemiluminescence Diagnostic," *AIAA 2003-4493, 39th AIAA/ASME/SAE/ASEE Joint Propulsion Conference and Exhibit*, Huntsville Alabama, July 20-23 2003.
16. J.M. Hall, M.J.A. Rickard, and E.L. Petersen, "Comparison of Characteristic Time Diagnostics for Ignition and Oxidation of Fuel/Oxidizer Mixtures Behind Reflected Shock Waves," *Combustion Science and Technology*, 177, pp. 455-483, 2005.
17. J.M. Hall and E.L. Petersen, "An Optimized Kinetics Model for OH Chemiluminescence at High Temperatures and Atmospheric Pressures," *International Journal of Chemical Kinetics*, 38 (12), pp. 714-724, 2006.
18. A.B. Barrett, S.C. Reehal and E.L. Petersen, "Measurement of Ignition Delay Time for a Syngas/Air Mixture Containing Water Vapor", *Proceedings from the Western States Section of the Combustion Institute 5th US Combustion Spring 2007 Meeting*, University of California San Diego, March 25-25, 2007.
19. T. Lieuwen, "Fuel Flexibility on Premixed Combustor Blowout, Flashback, Autoignition, and Stability," GT2006-90770, *Proceedings from ASME Turbo Expo*, Barcelona, Spain, June 6-9, 2006.
20. C.J. Aul, J. de Vries, E.L. Petersen, "New Shock-Tube Facility for Studies in Chemical Kinetics at Engine Conditions," *Proceedings from the Eastern States Fall Technical Meetings*, University of Virginia, October 21-25, 2007.
21. E.L. Petersen, "On the Use of Endwall Emission as a Shock-Tube Ignition Diagnostic," *Proceedings from the Western States Section of the Combustion Institute 5th US Combustion Spring 2007 Meeting*, University of California San Diego, March 25-25, 2007.